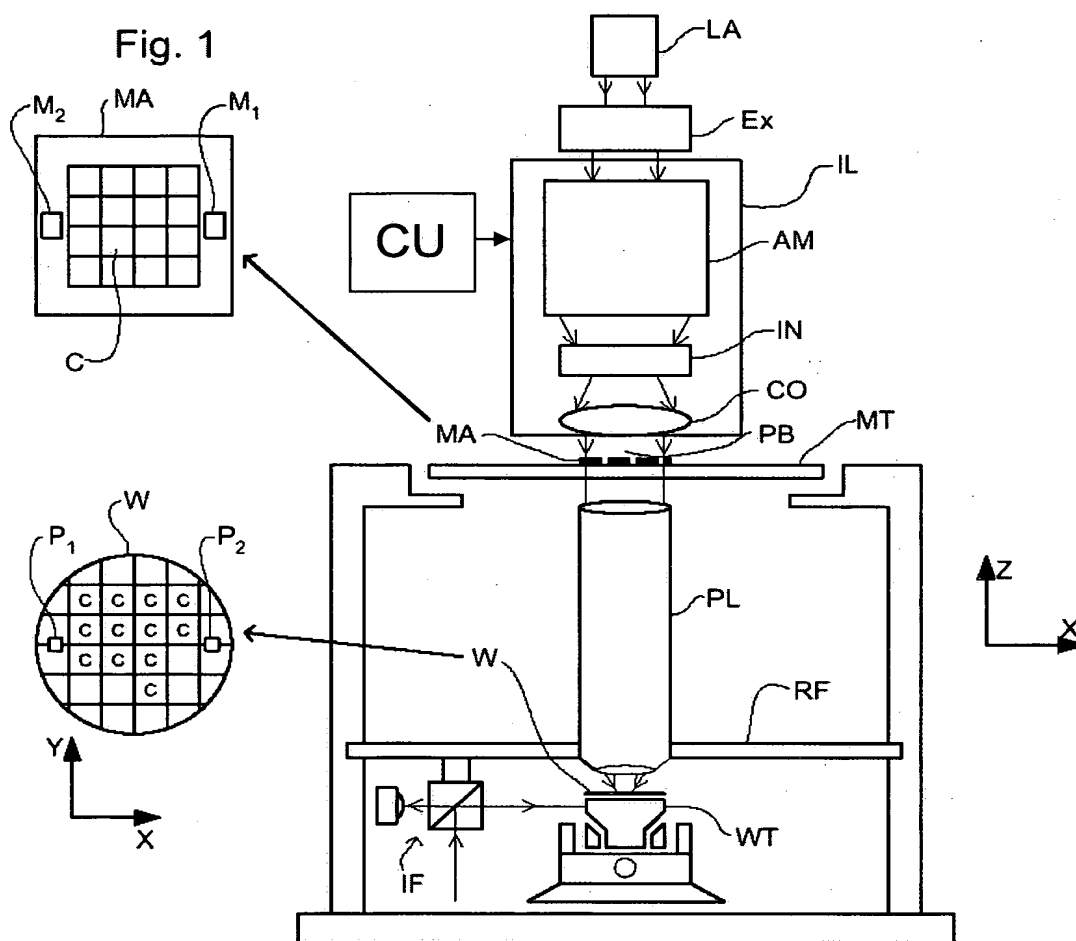


Fig. 1



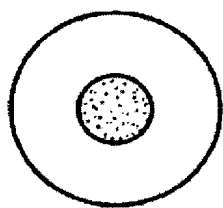


FIG. 2

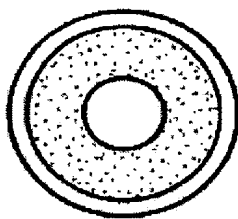


FIG. 3

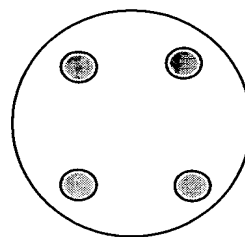


FIG. 4

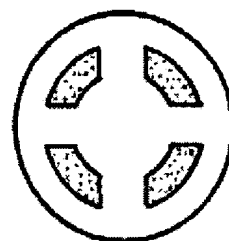


FIG. 5

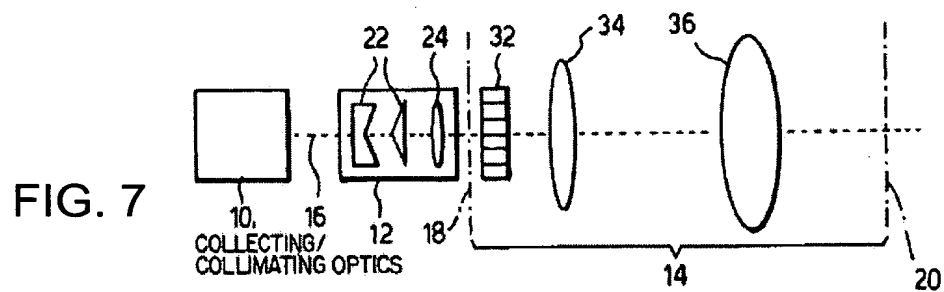
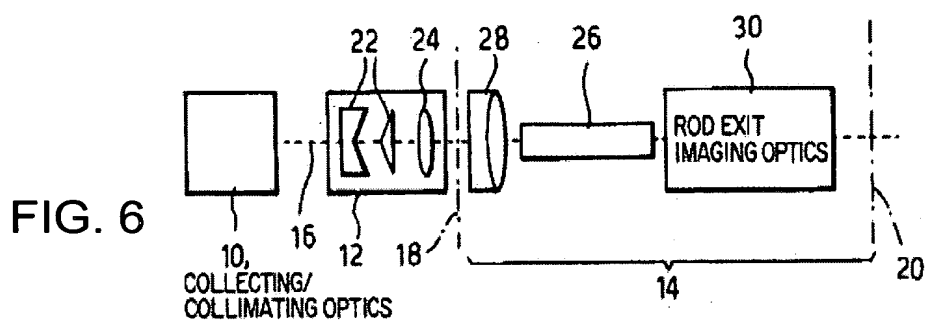


FIG. 8

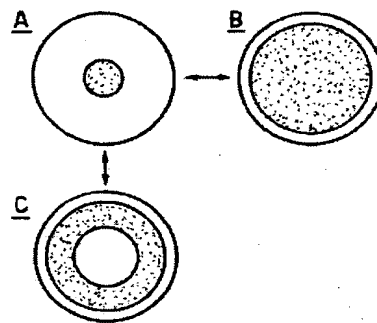
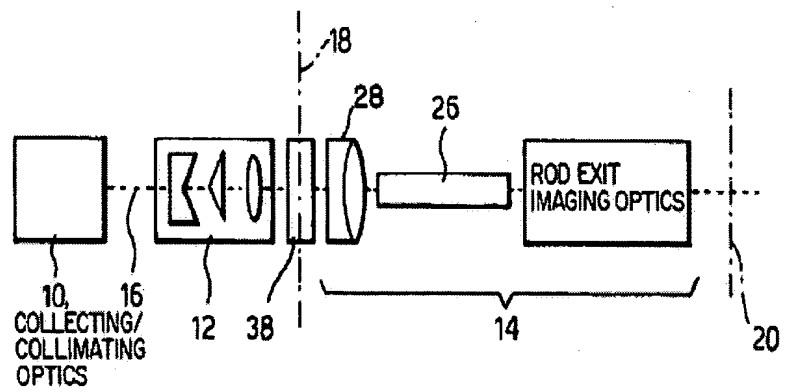


FIG. 9



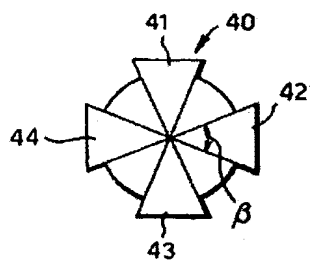


FIG. 10a

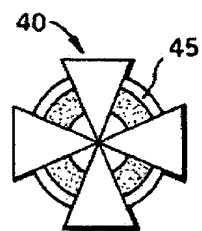


FIG. 10b

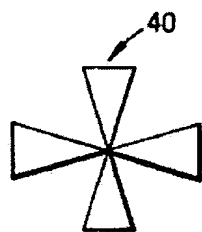


FIG. 11

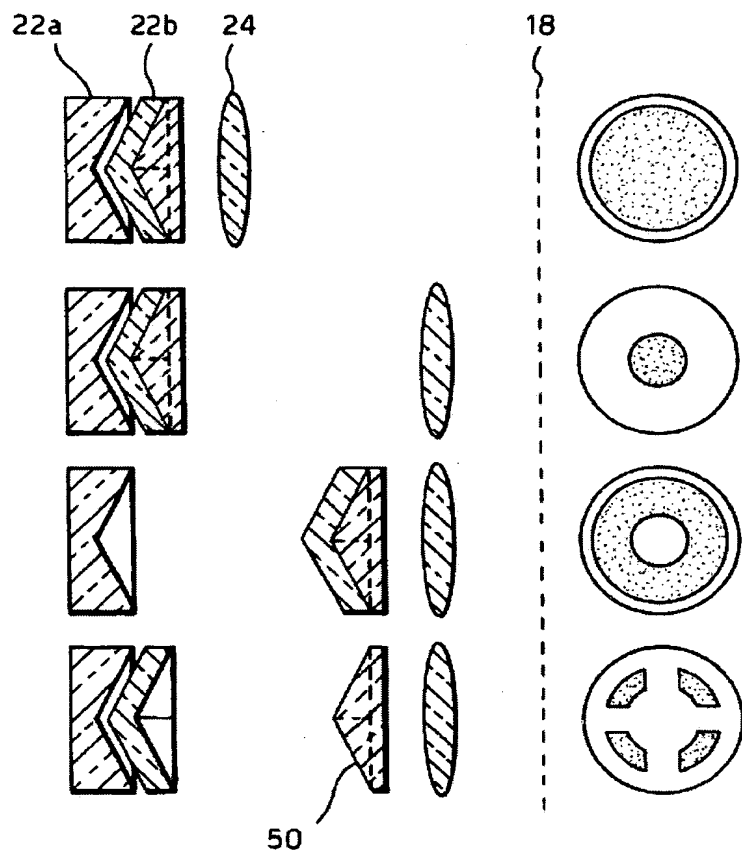


FIG. 12

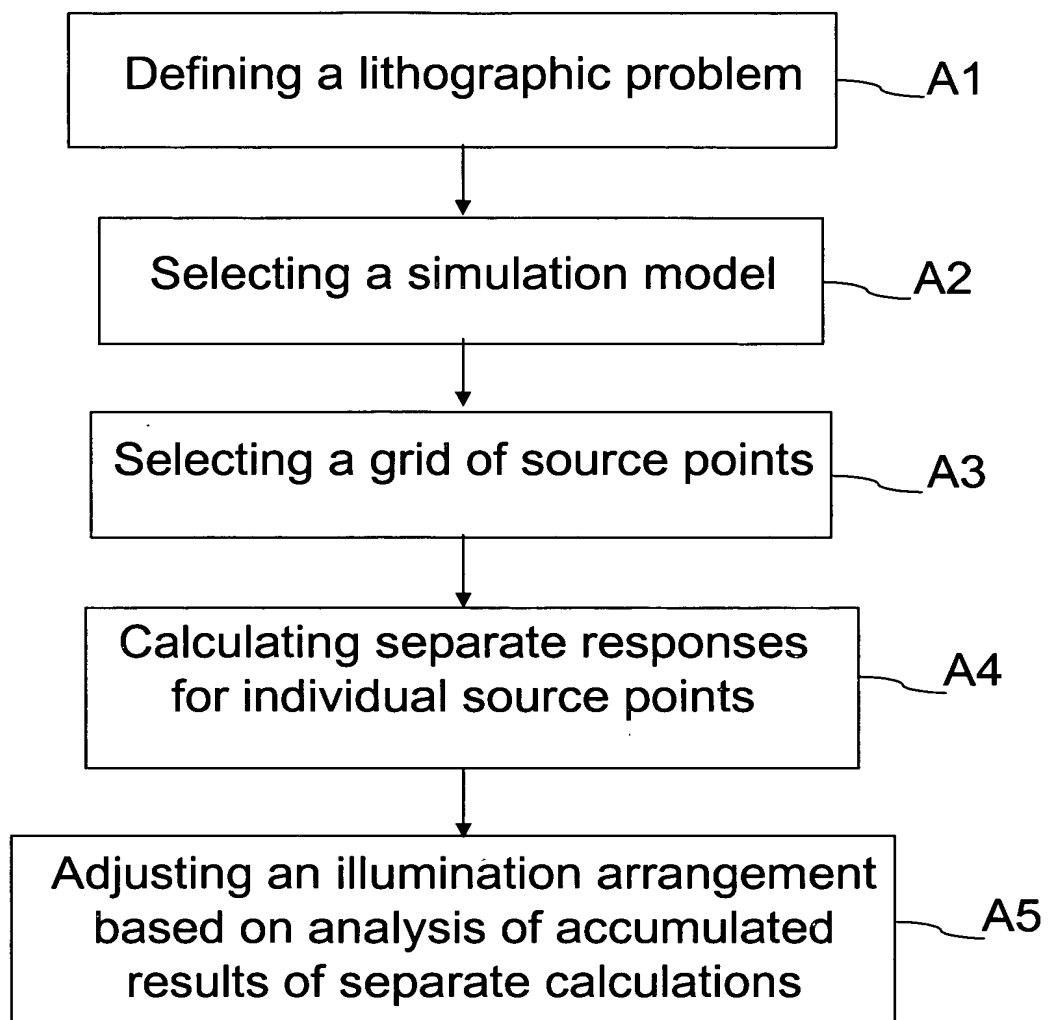
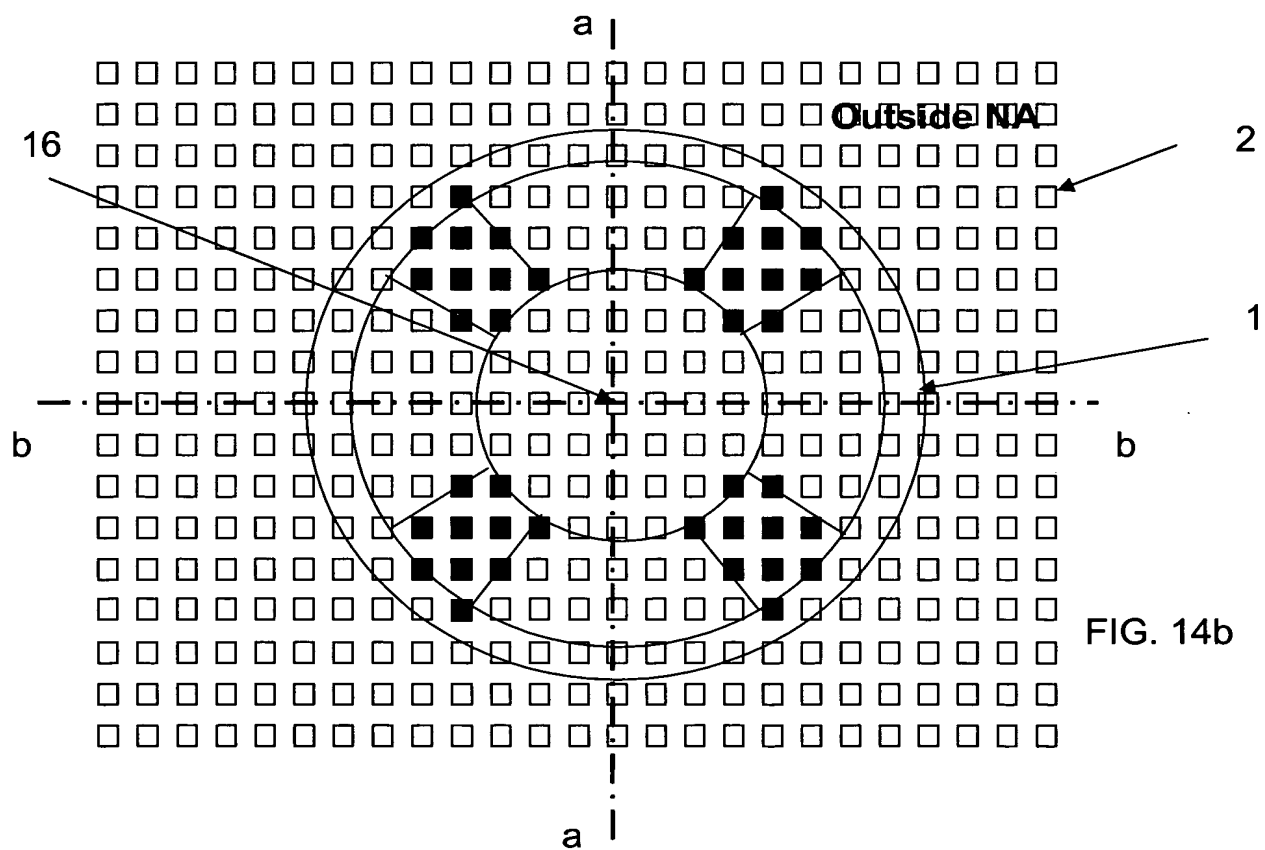
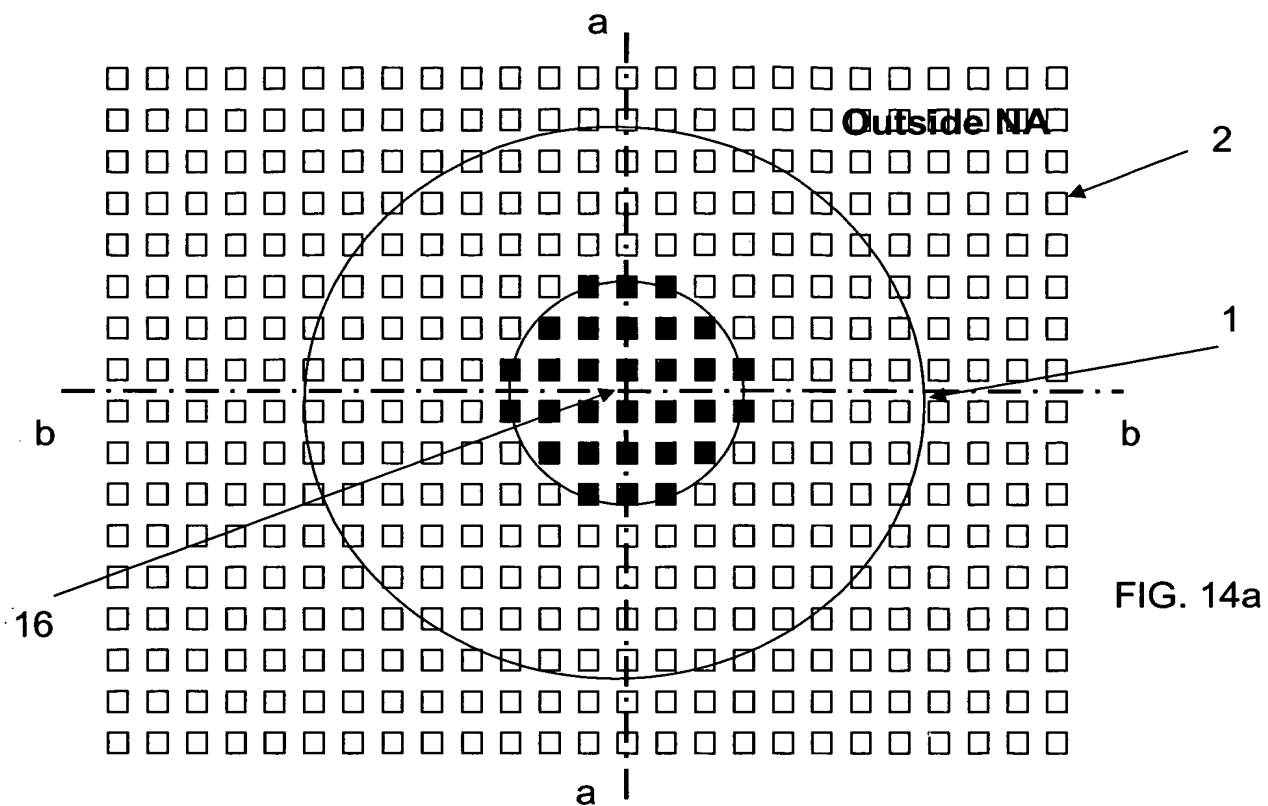


FIG. 13



65nm CPL isolated lines, 193nm
0.85NA, scalar aerial image simulations
0.2 μ m defocus

high DOF expected with
appropriate Quasar

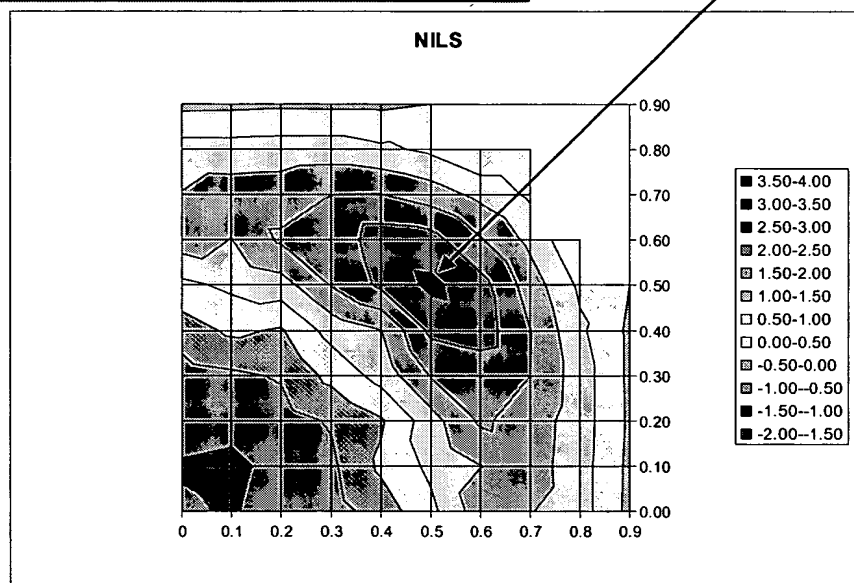


FIG. 15

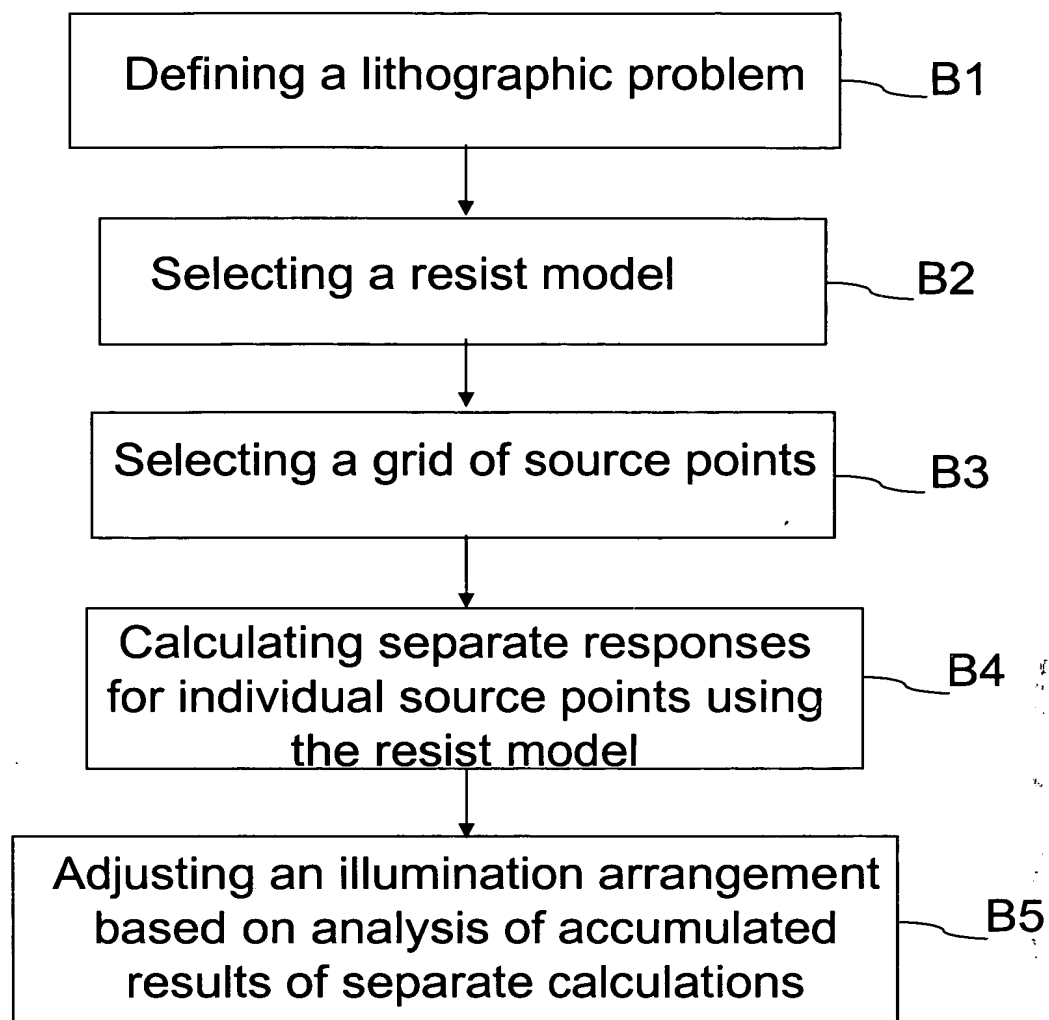


FIG. 16

65nm CPL isolated lines, 193nm
0.85NA, TOK63 vector resist simulations

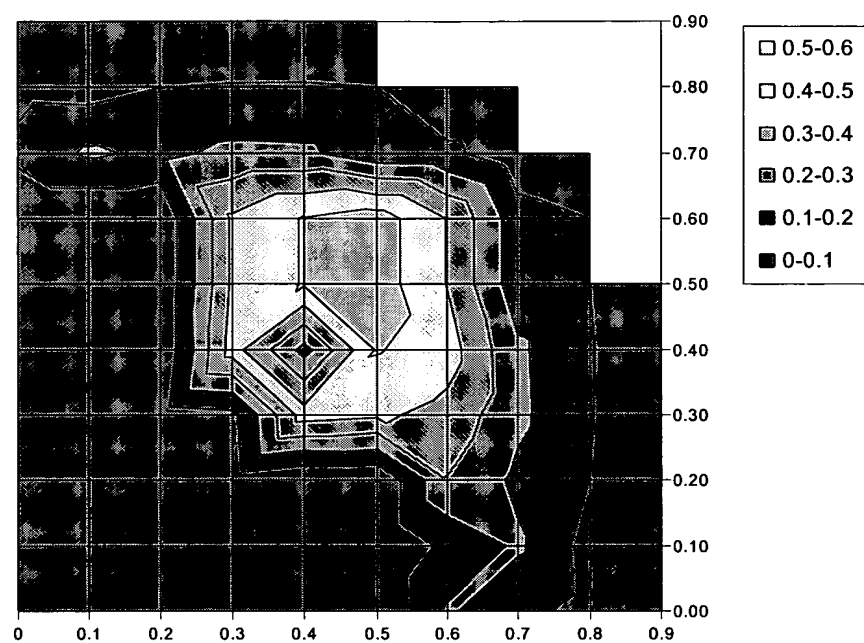


FIG. 17

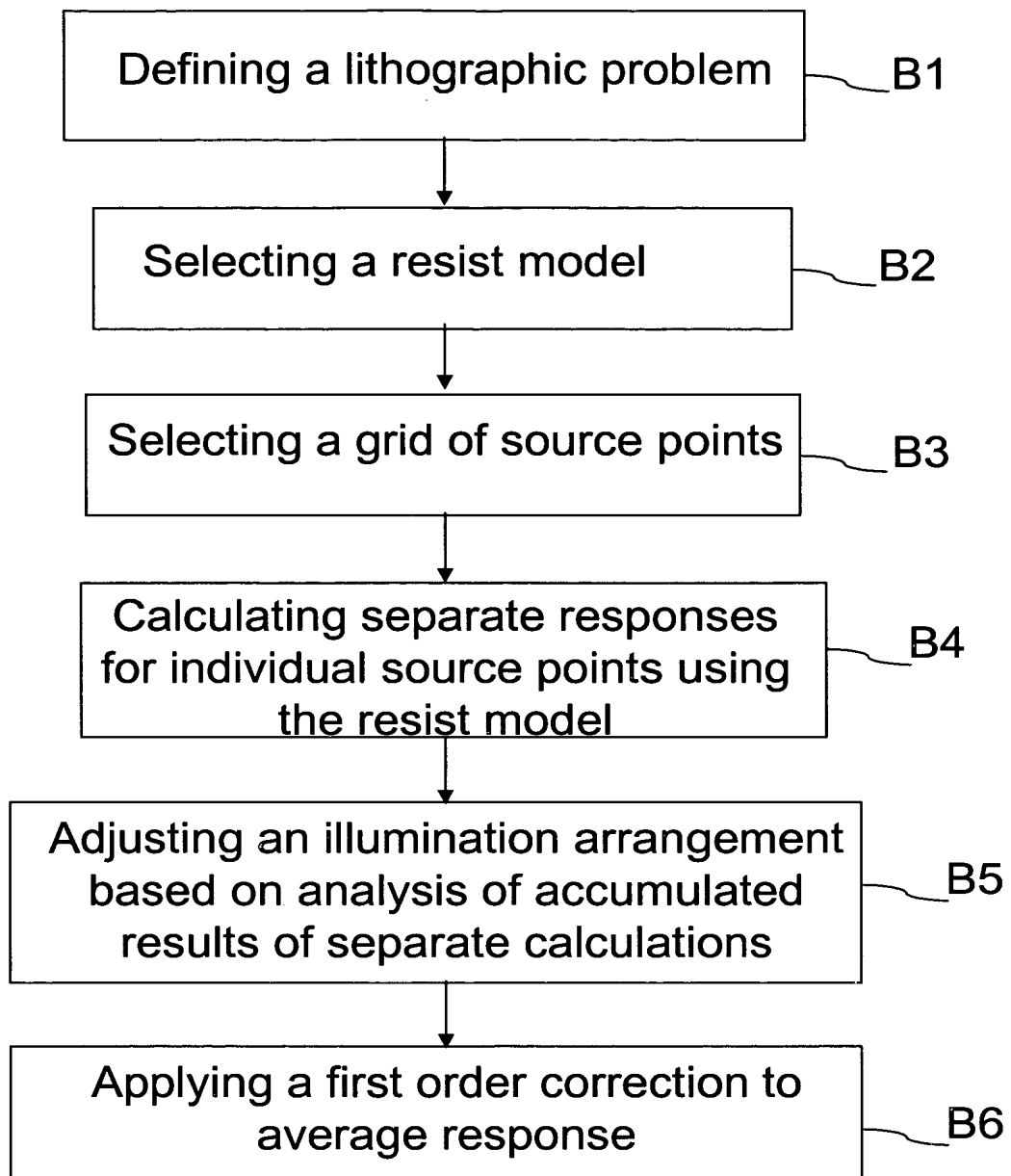


FIG. 18

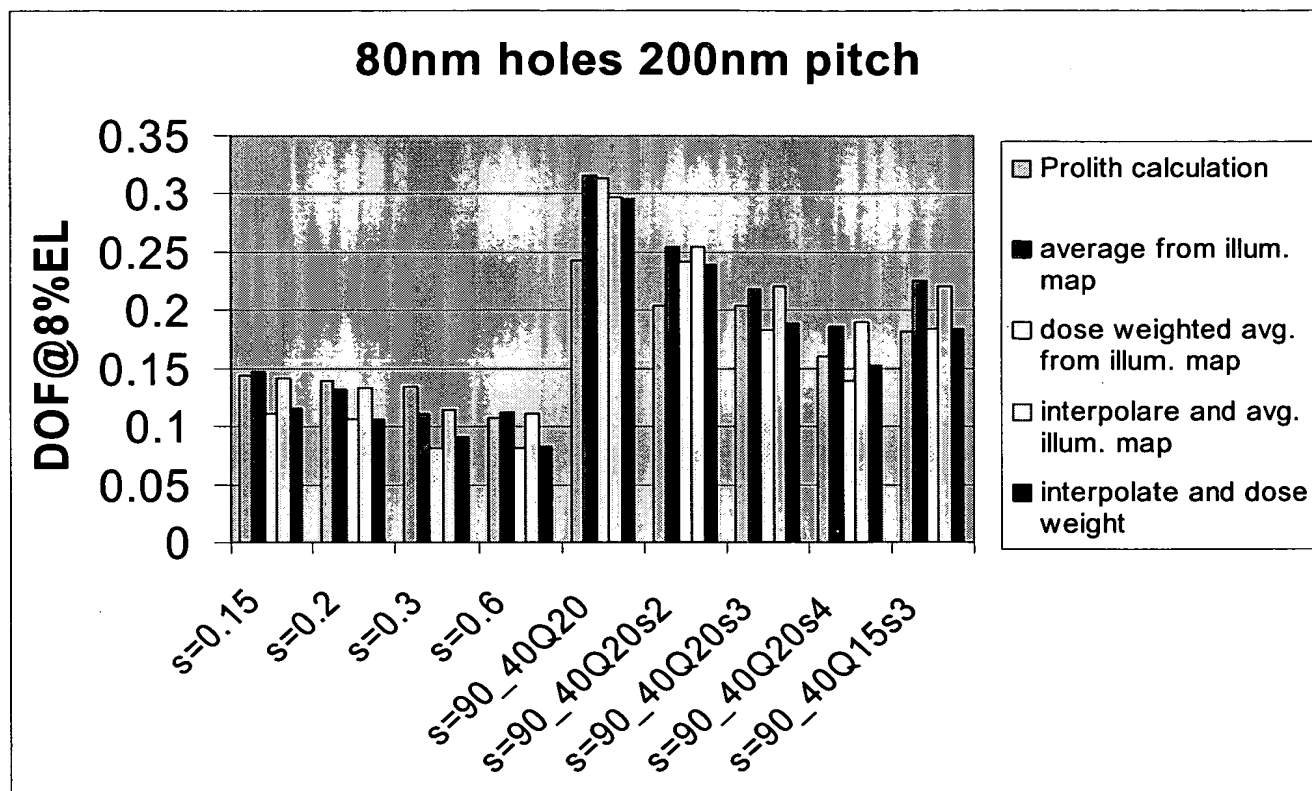
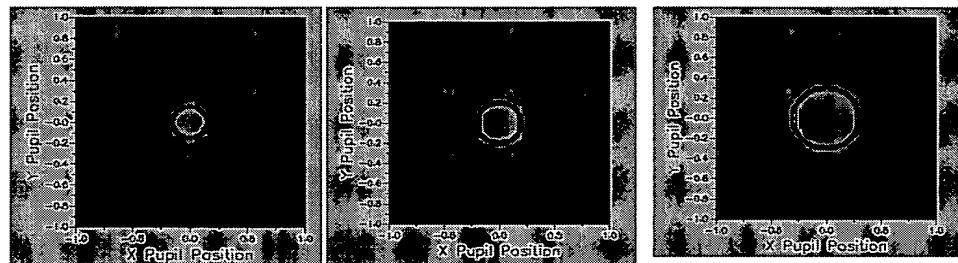
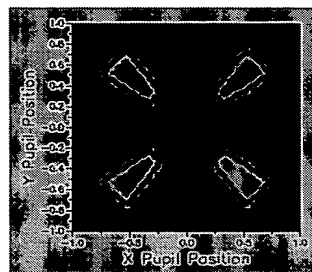


FIG. 19

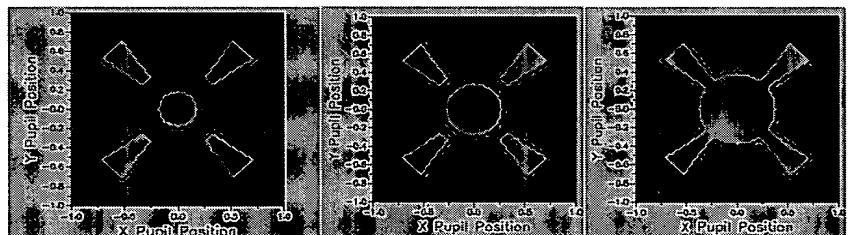
- 0.15, 0.2, 0.3, 0.6 σ conv



- 0.9/0.4 Q20



- 0.2, 0.3, 0.4 σ + 0.9/0.4 Q20



- 0.3 σ + 0.9/0.4 Q15

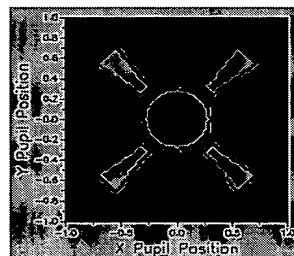


FIG. 20

trial illuminator	prediction based on weighted and interpolated source measurements	Prolith simulation with this illuminator
0.85_0.55Q30	0.293u	0.23u
0.75_0.55Q20	0.416	0.41
0.80_0.60Q20	0.383	0.355
0.80_0.60annular	0.110	0.10
0.75_0.55annular	0.118	0.105

FIG. 21

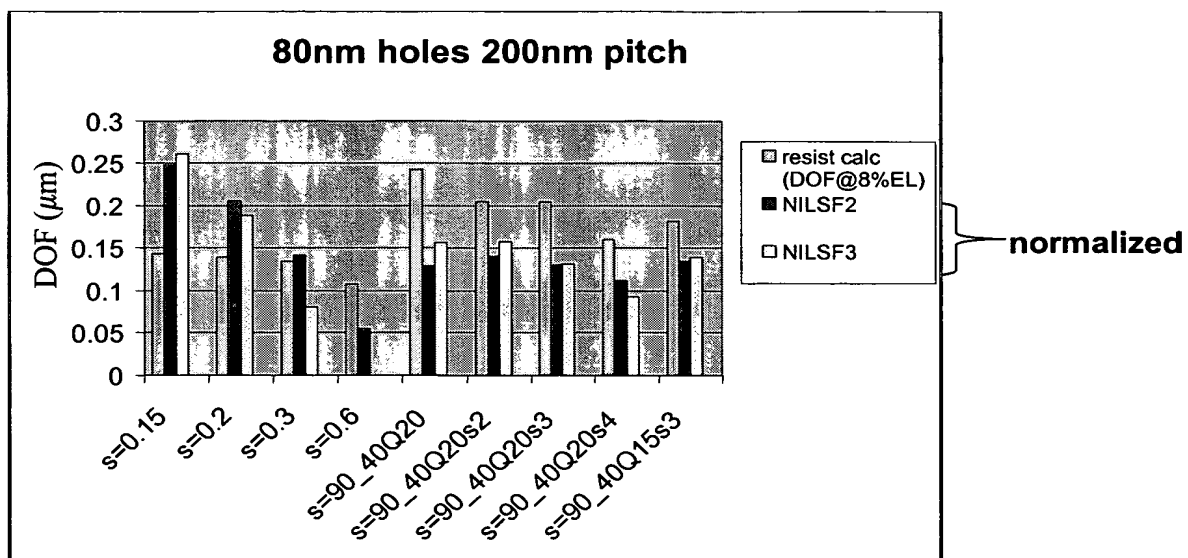


FIG. 22

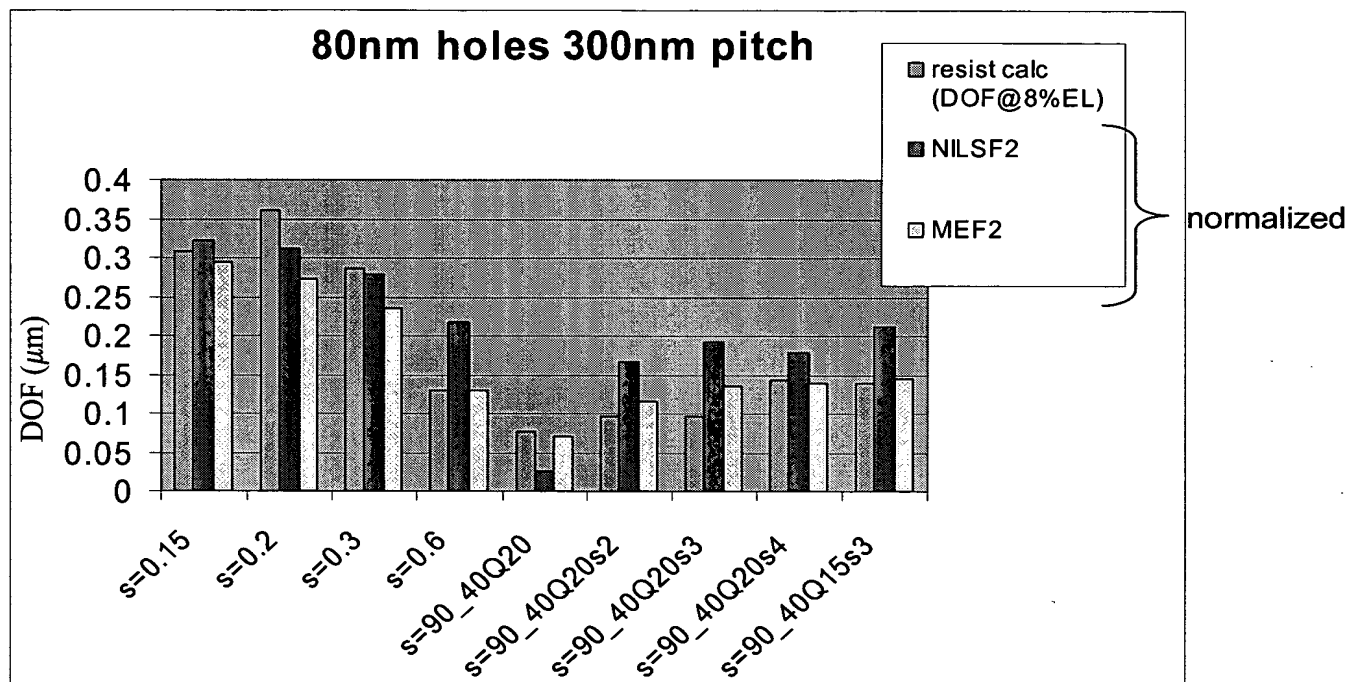


FIG. 23

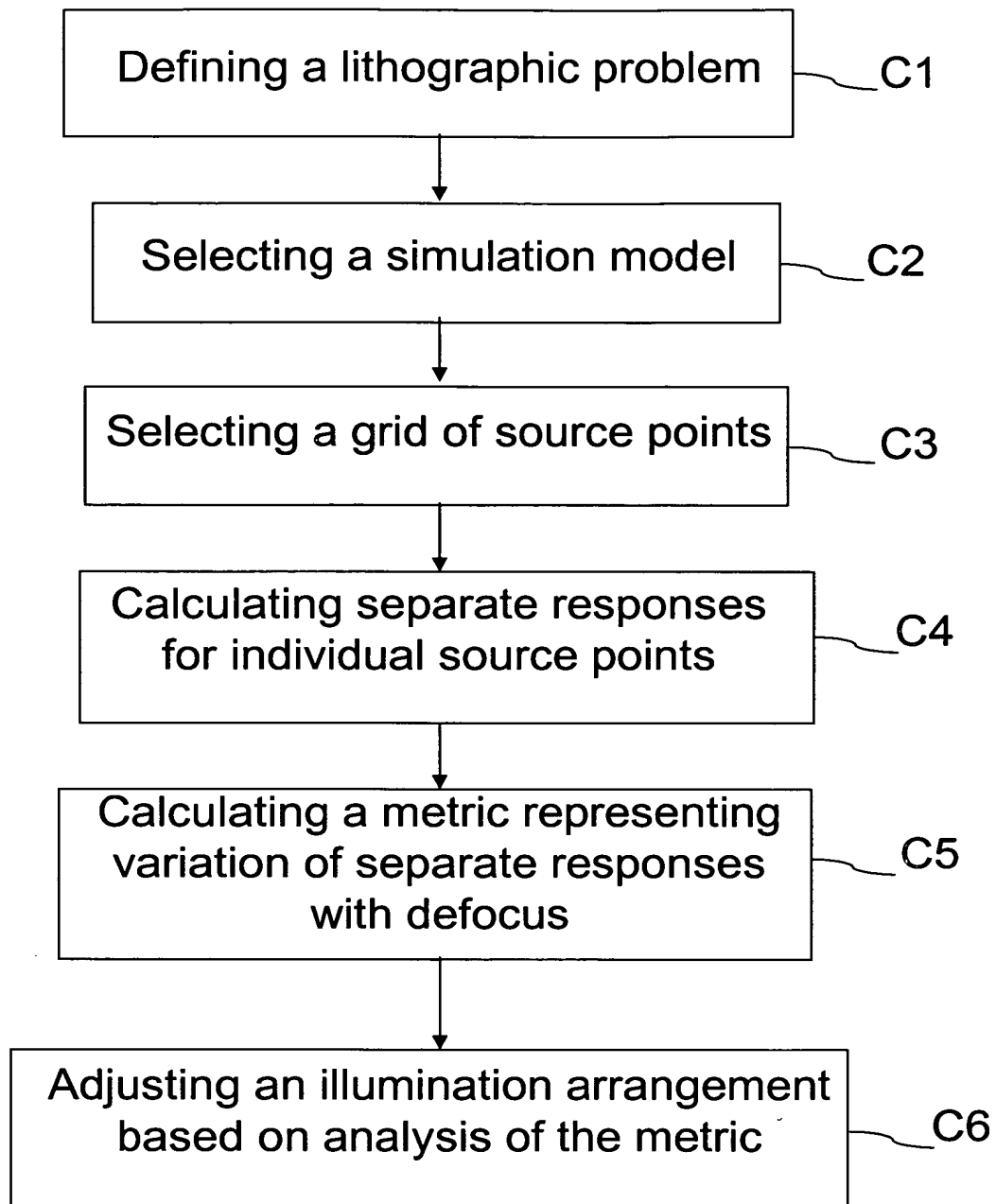


FIG. 24

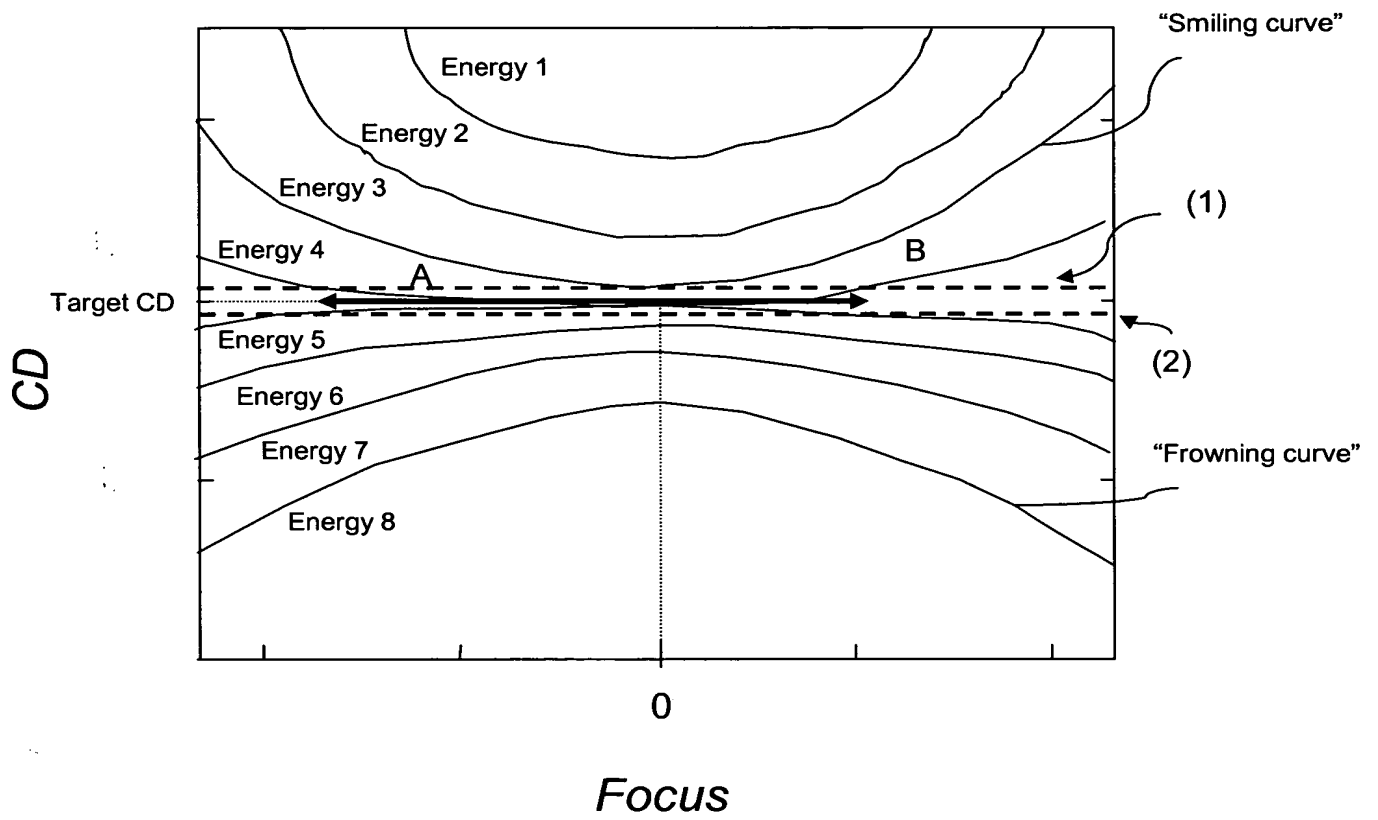
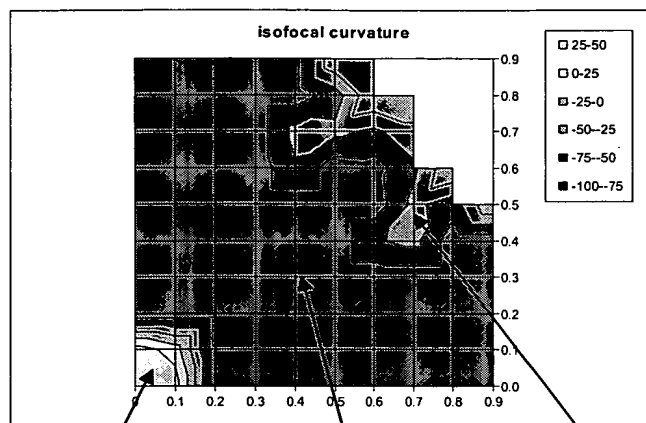


FIG. 25

resist calculation $CD(BF+0.2)-CD(BF)$

FIG. 26a



Area where
Bossung
"smiles"
 $CD(=0.2) > C$
 $D(f=0)$

Area where
Bossung
"frowns" severely
hole closed at
0.2u defocus

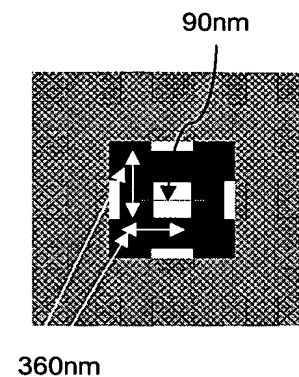
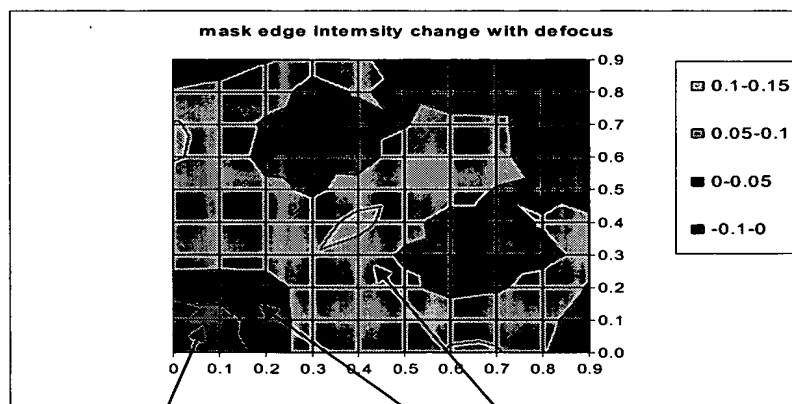


FIG. 26c

Area where
Bossung
"frowns"
less
severely

Aerial image calculation $\text{thresh}(BF) - \text{thresh}(BF+0.2)$

FIG. 26b

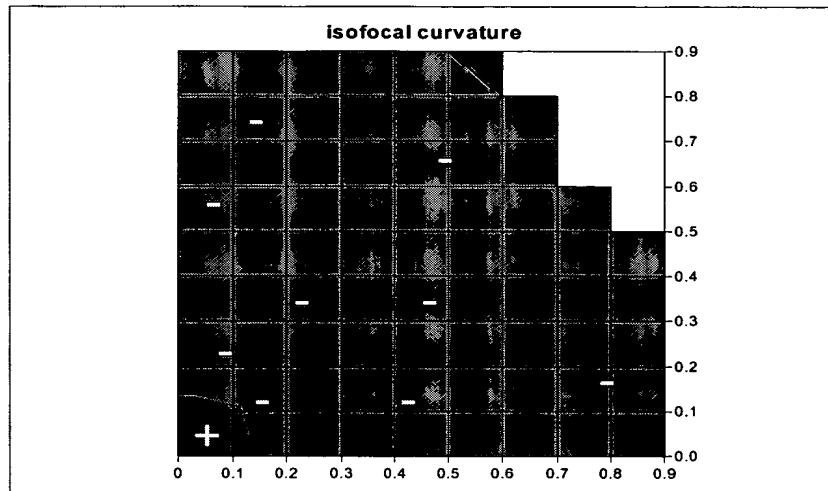


Area where
image CD is
larger in
defocus

Area where
image CD is
smaller in
defocus

resist calculation $CD(BF+0.2)-CD(BF)$

FIG. 27a



Aerial image calculation $\text{thresh}(BF)-\text{thresh}(BF+0.2)$

FIG. 27b

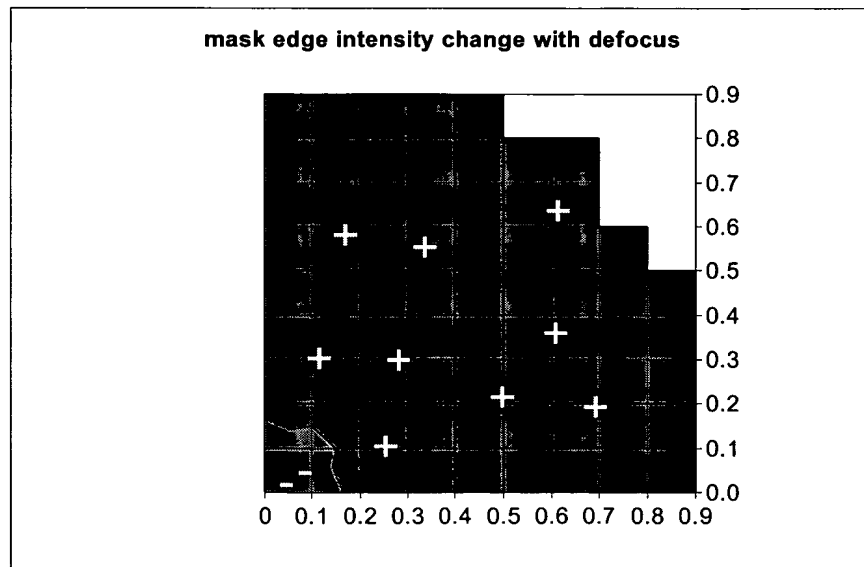
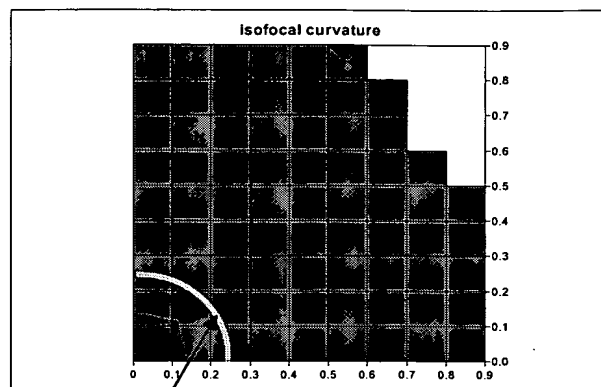


FIG. 28



$\sigma=0.25$ combines areas of + and - isofocal curvature

At $\sigma=0.25$, process is approximately isofocal. DOF is good but dose latitude is low.

FIG. 29

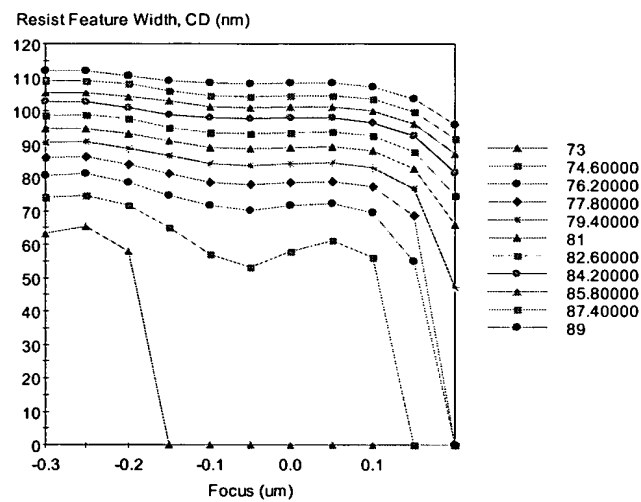
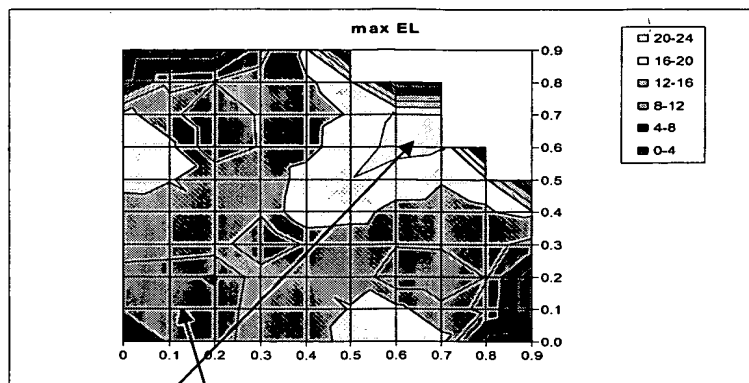


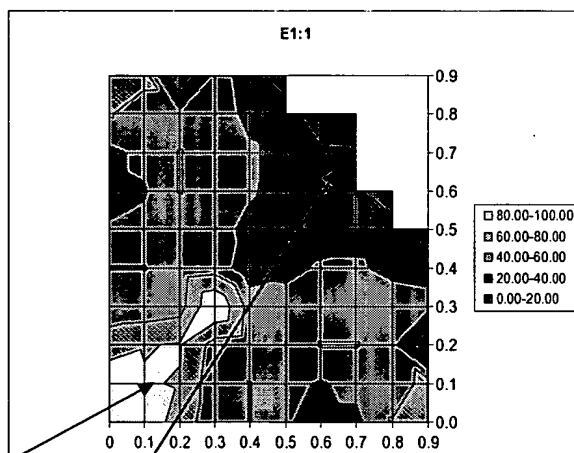
FIG. 30a



Low σ area provides poor EL and also requires high dose to print (weak aerial image)

Desirable area for high EL is wide quasar

FIG. 30b



Low σ area provides poor EL and also requires high dose to print (weak aerial image)

Wide quasar also provides low E1:1 (strong aerial image)

$$\text{Illuminator} = \sigma(0.1 \text{ conv}) + (0.92/0.88Q5^\circ)$$

FIG. 31

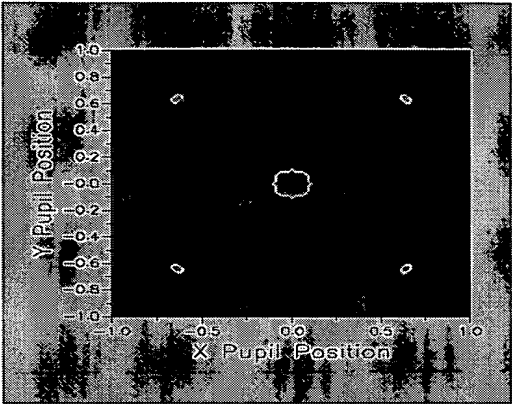


FIG. 32

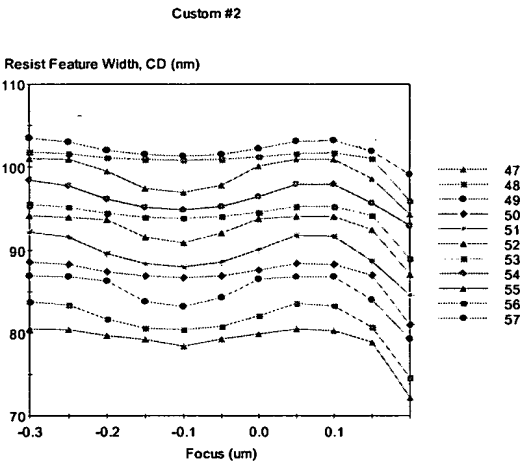
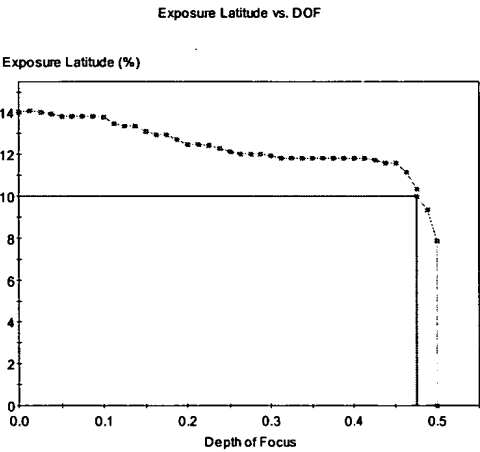


FIG. 33



optimization method	illumination	max EL	max DOF	DOF @ 10% EL	DOF @ 5% EL
standard	0.95/0.70Q30*	18%	0.3	0.18	0.24
simple isofocal compensation	0.25 conv	8%	>0.55	0	0.29
high EL isofocal compensation	0.92/0.88Q5*+0.1conv	16%	>0.65	0.57	0.63

FIG. 34

Large improvement in process window may be possible by appropriate use of illuminator to compensate isofocal curvature

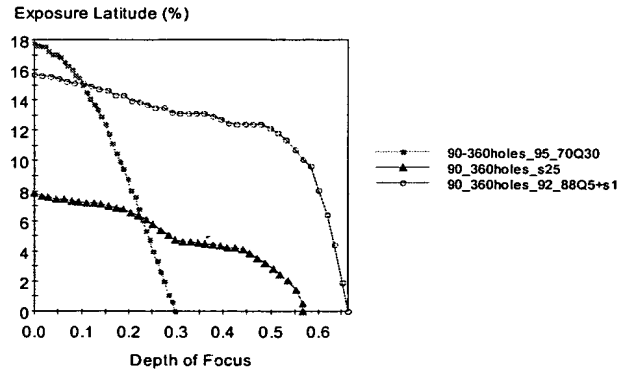


FIG. 35a

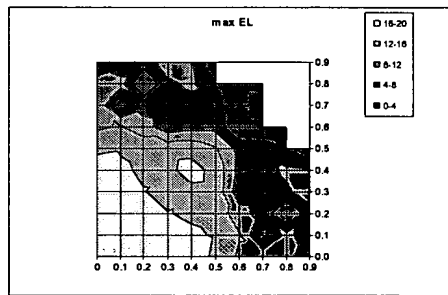


FIG. 35b

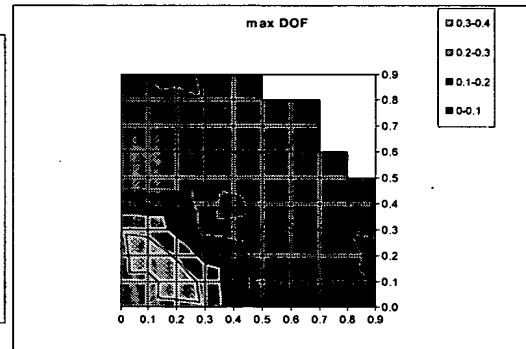


FIG. 35d

FIG. 35c

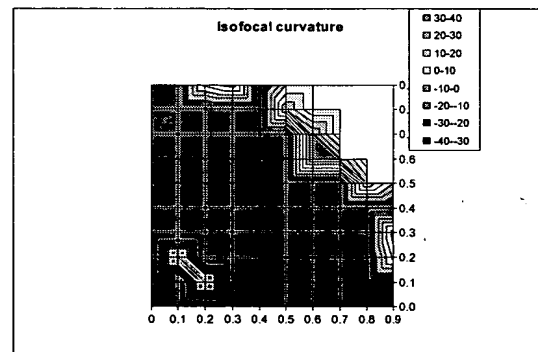
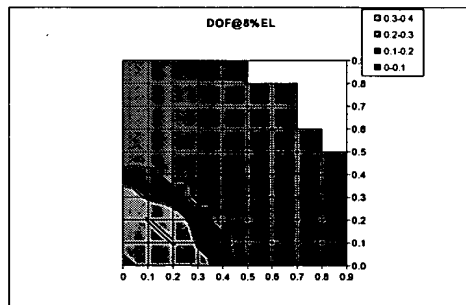


FIG. 36a

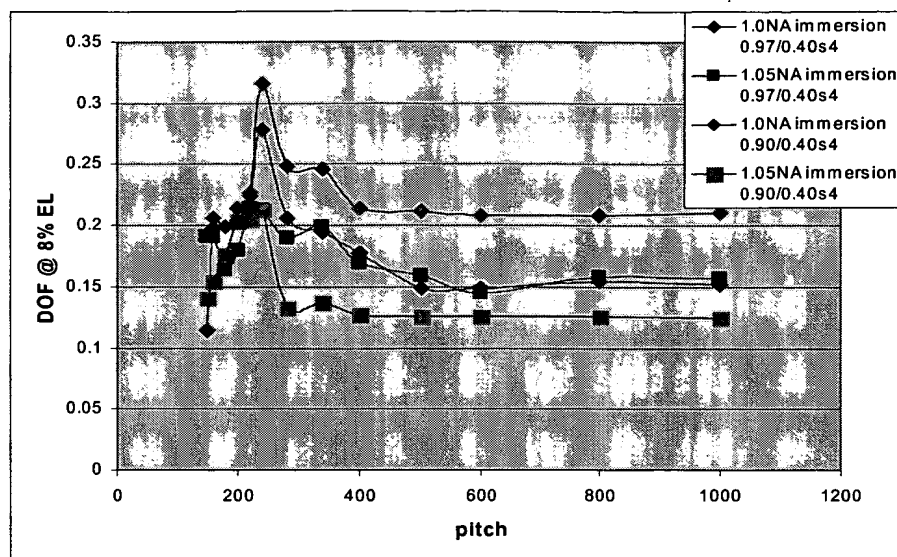
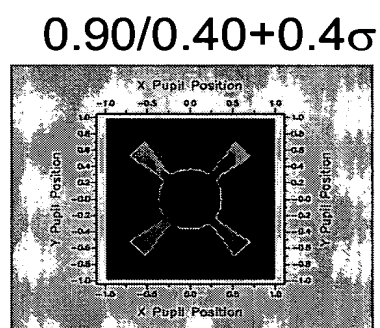


FIG. 36b



0.97/0.40+0.4 σ

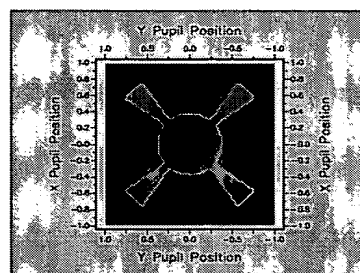


FIG. 36c

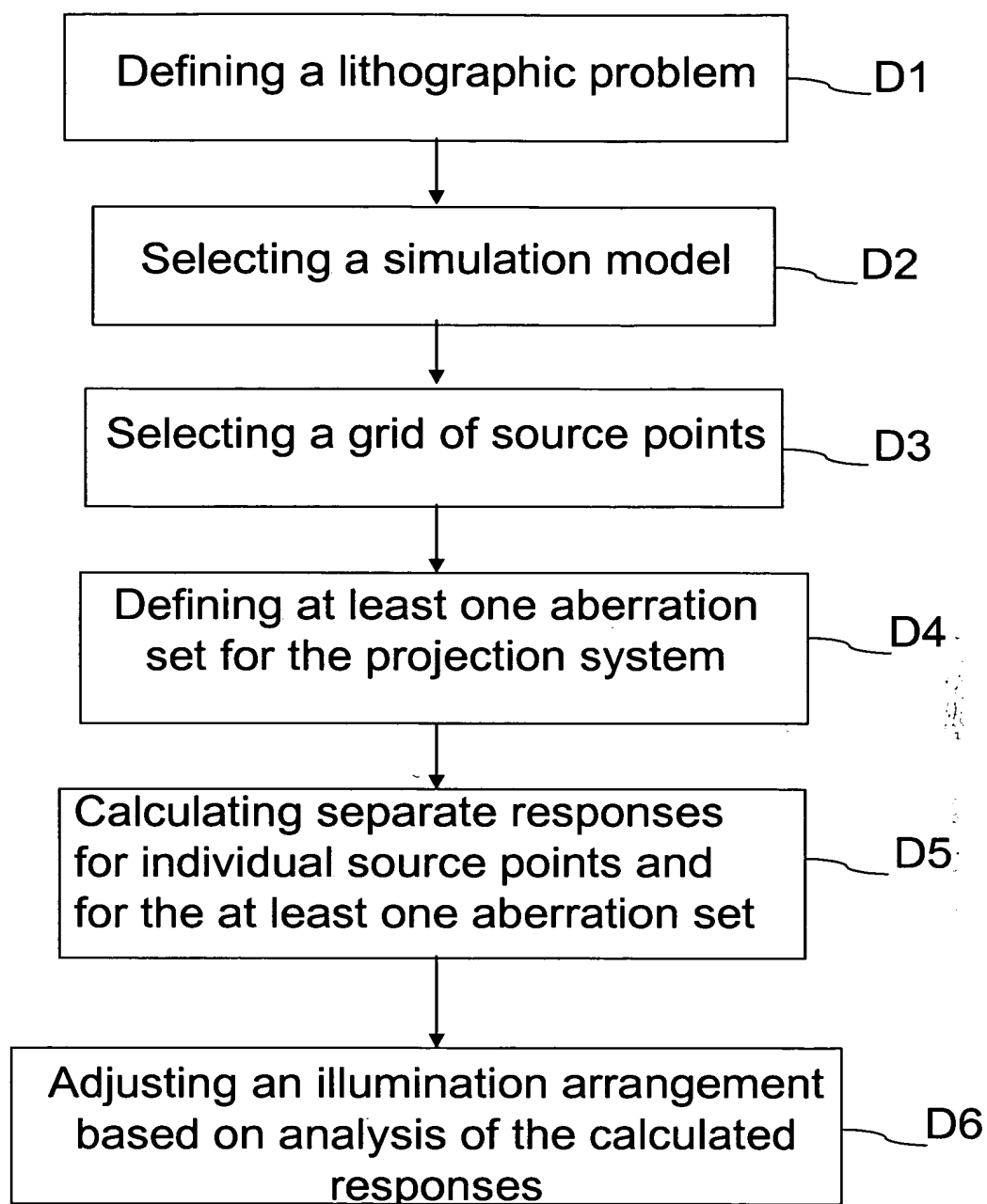


FIG. 37

Under these conditions, the structure
is very aberration sensitive

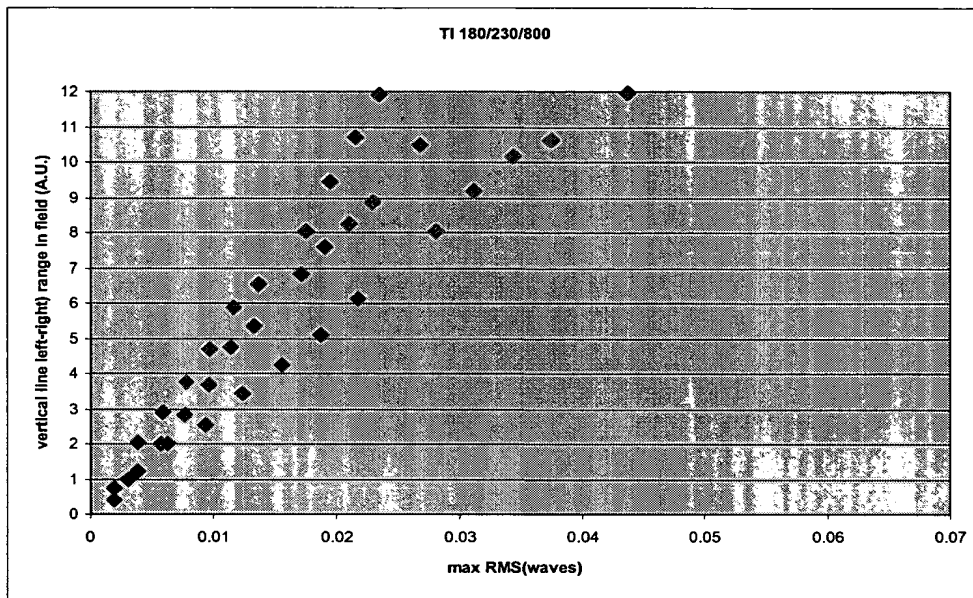


FIG. 38a

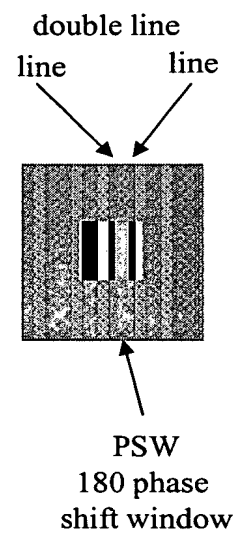


FIG. 38b

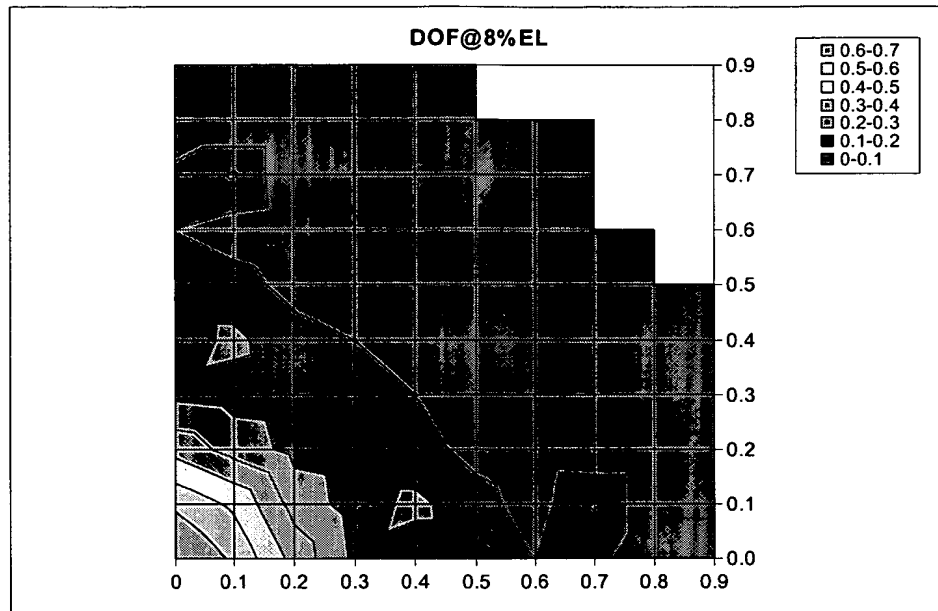


FIG. 39a

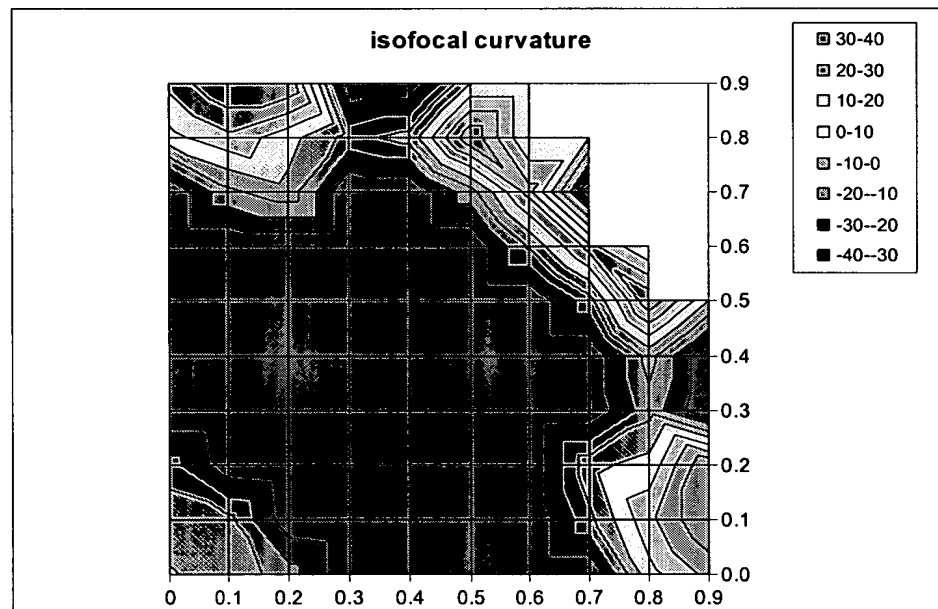
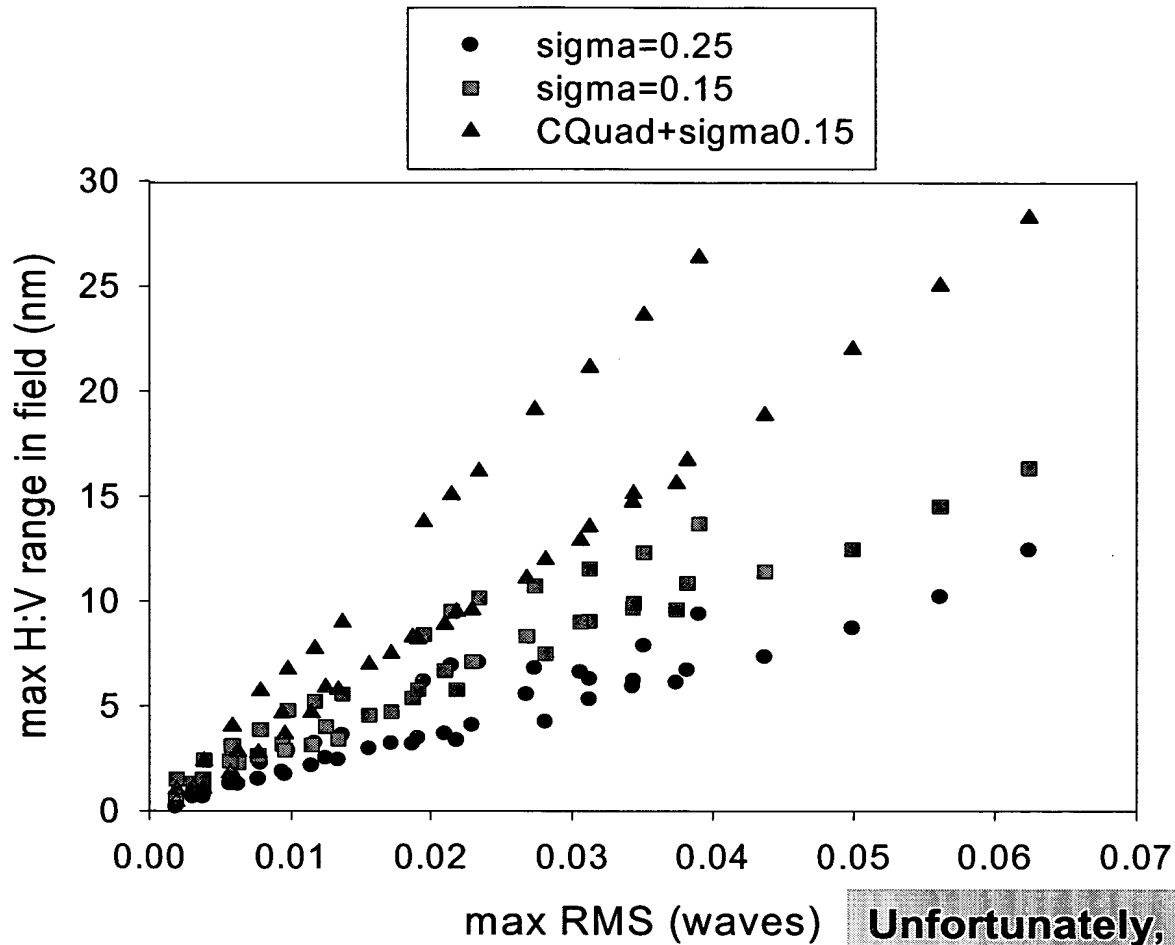


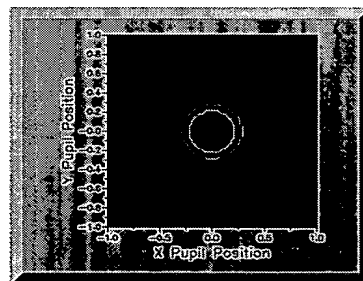
FIG. 39b

Illuminator comparison for double line

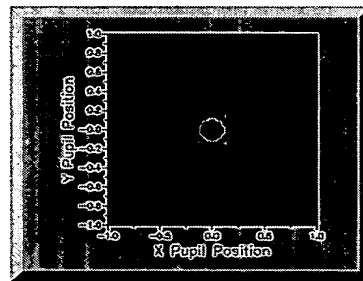


Unfortunately, the alternate settings have higher aberration sensitivity.

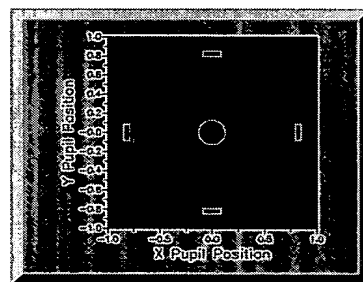
FIG. 40



$\sigma=0.25$



$\sigma=0.15$



$\sigma=0.15 +$
small Cquad

FIG. 41

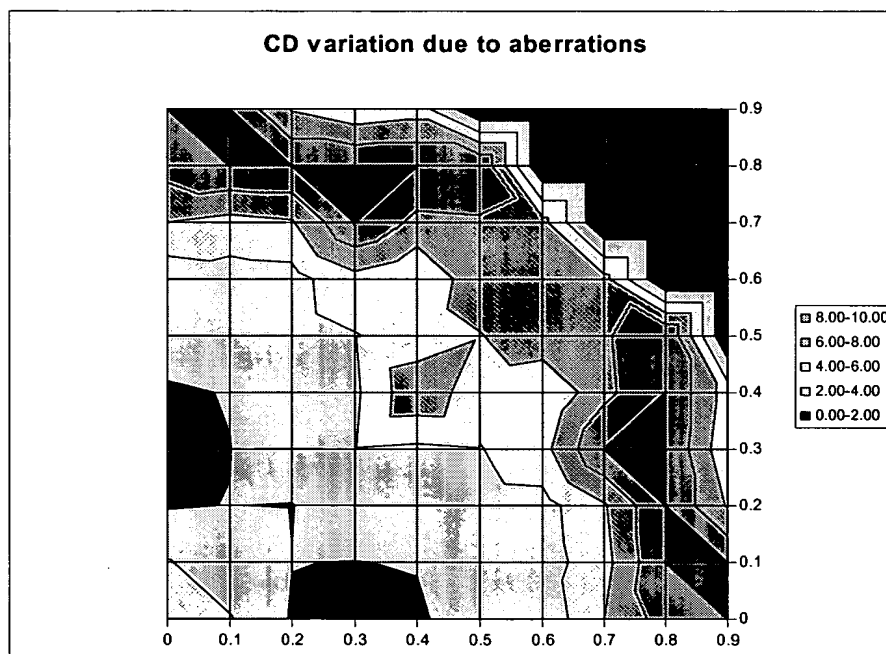
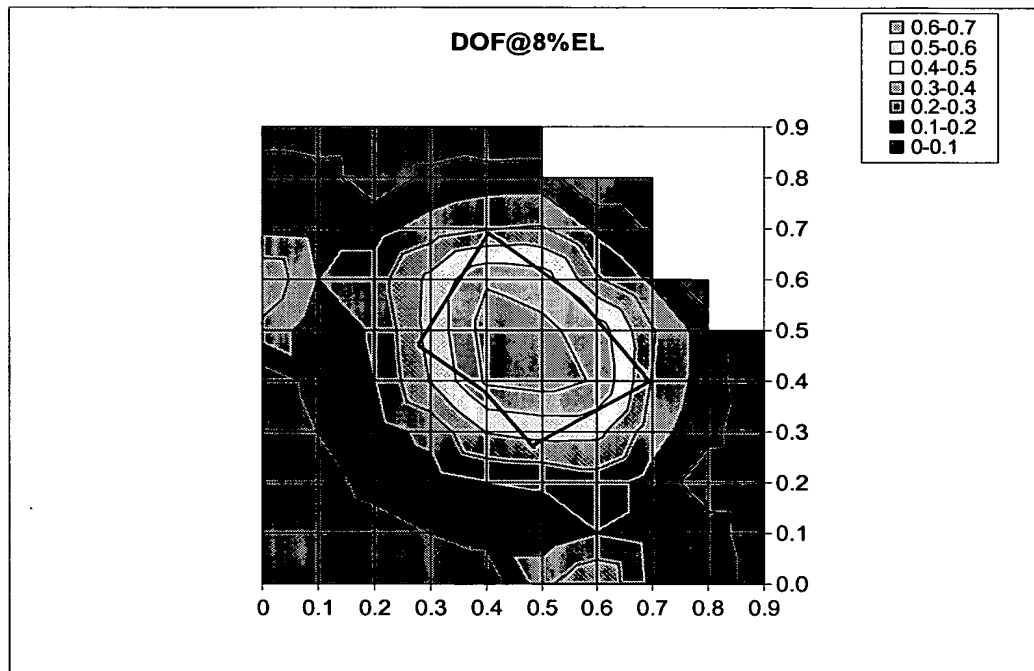


FIG. 42

Illum. Optimization with 0.75NA



tight Quasar looks best
 $\Rightarrow 0.80/0.55Q30^\circ$

FIG. 43

Source visualization of aberration sensitivity

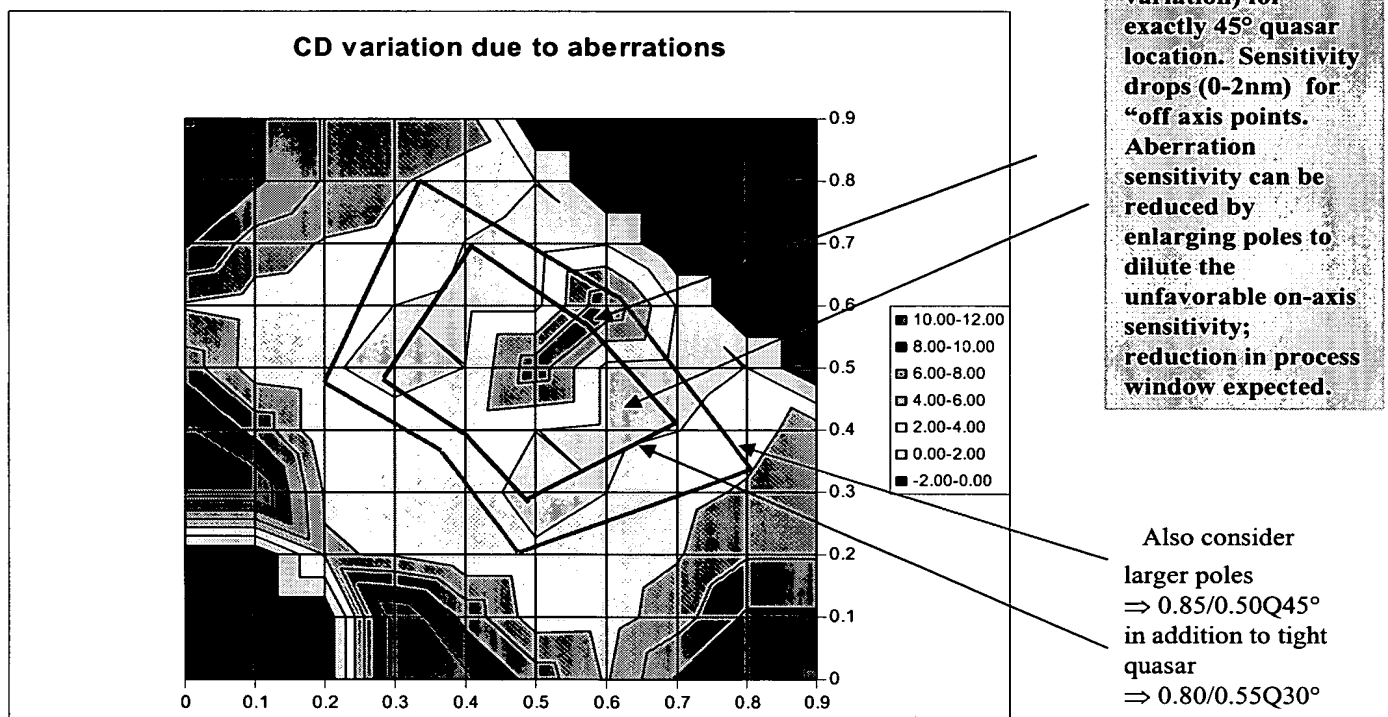


FIG. 44

Illuminator comparison for double line

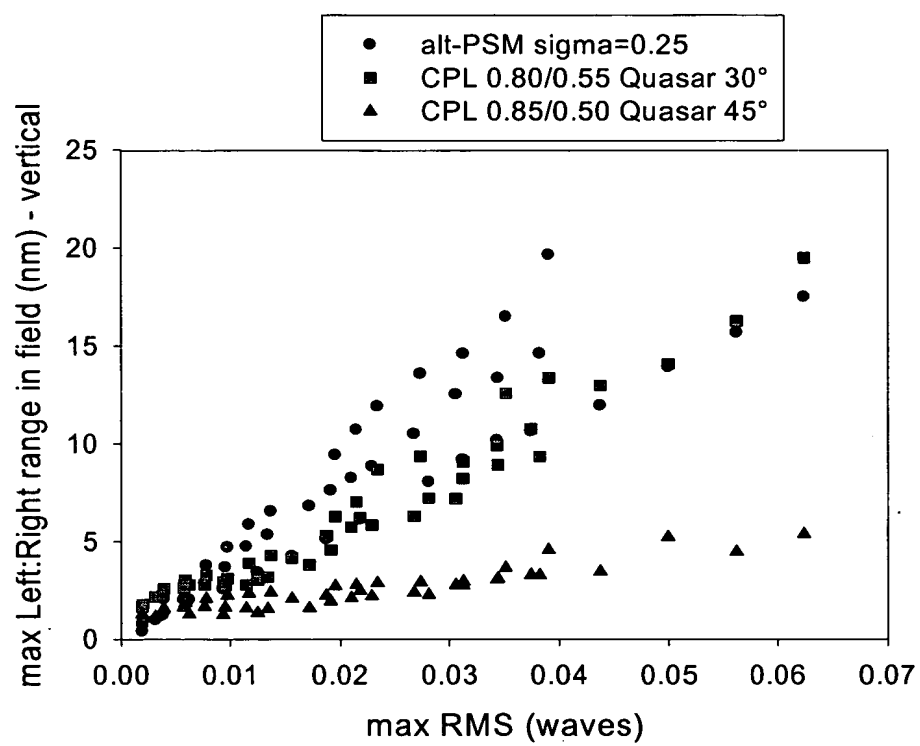


FIG. 45

CPL with reduced aberration sensitivity
increased pole size still gives favorable process window

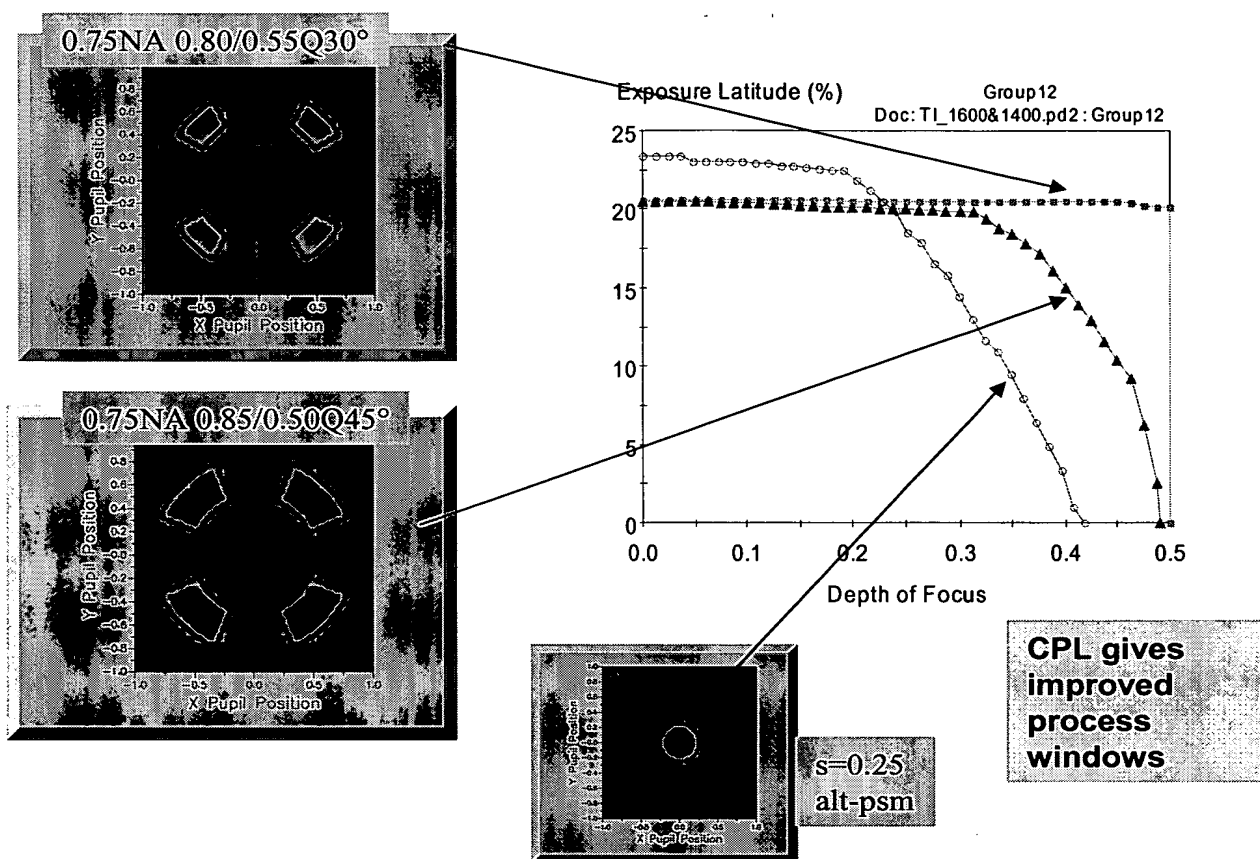


FIG. 46

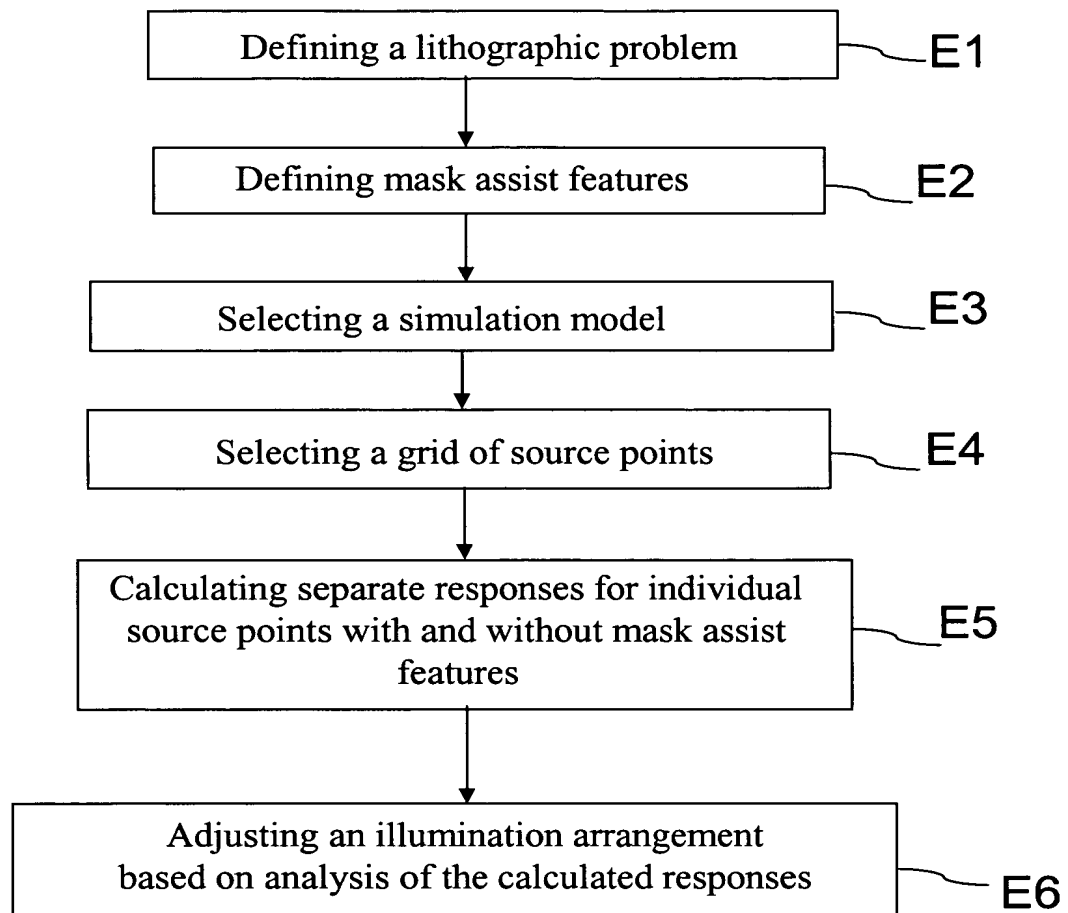


FIG. 47

6%Att-PSM, 1 Anti-Scattering Bar (ASB)/side
50nm ASB, 150nm pitch

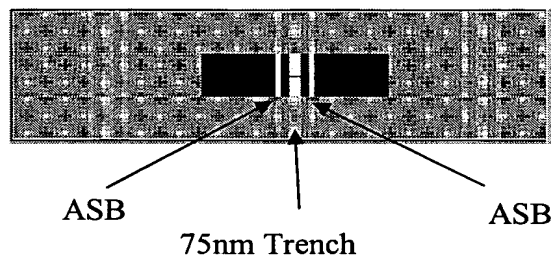


FIG. 48

Optimization
requires very wide
CQuad or quasar

75nm trench, 15nm bias
6% att-psm, 193nm 0.93NA

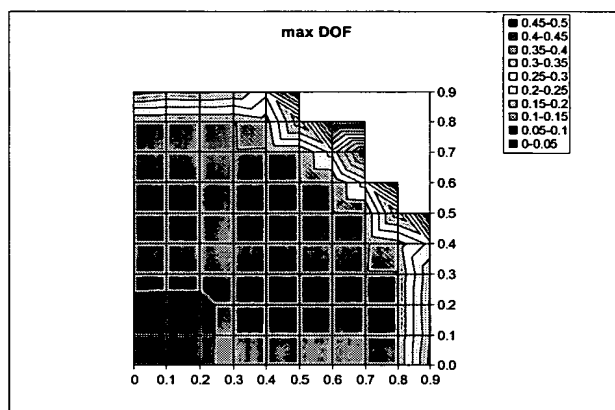


FIG. 49a

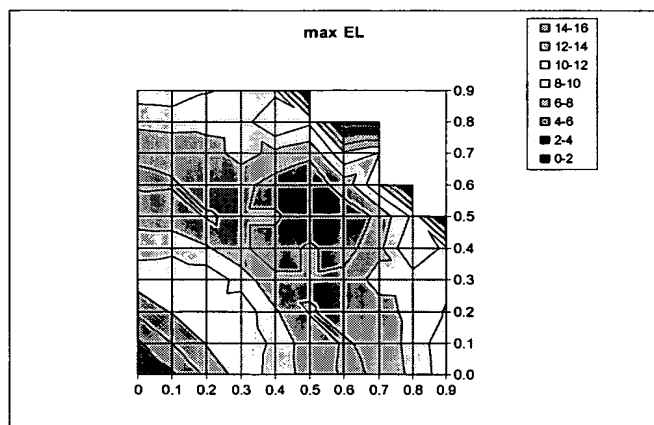


FIG. 49b

75nm trench, 15nm bias
6% att-psm, 193nm 0.93NA

1SB / side


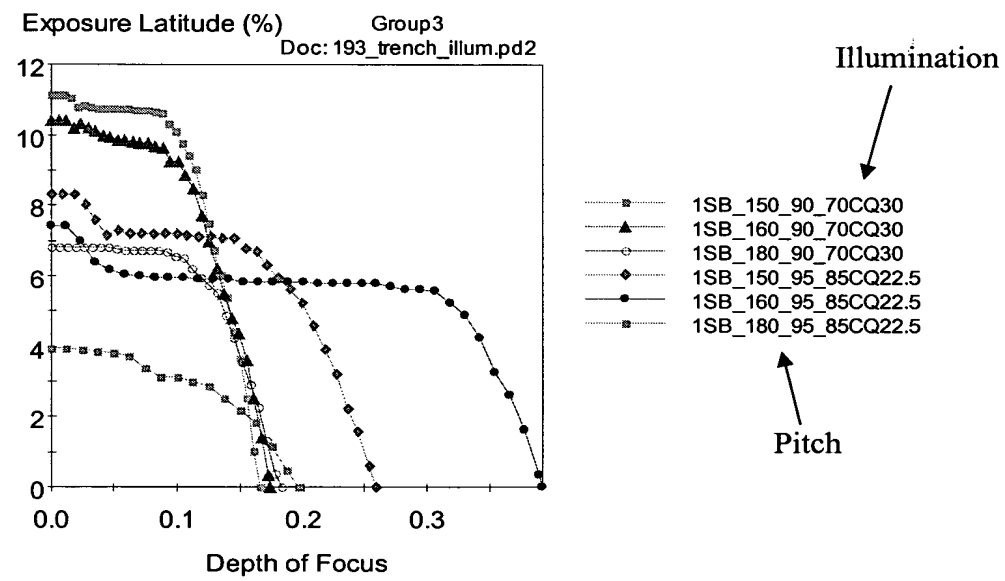
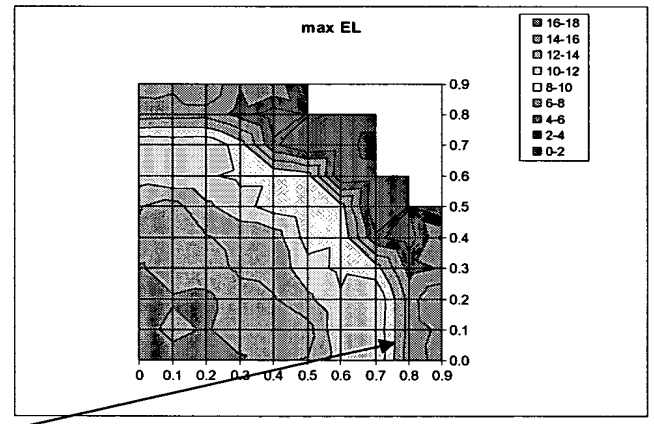
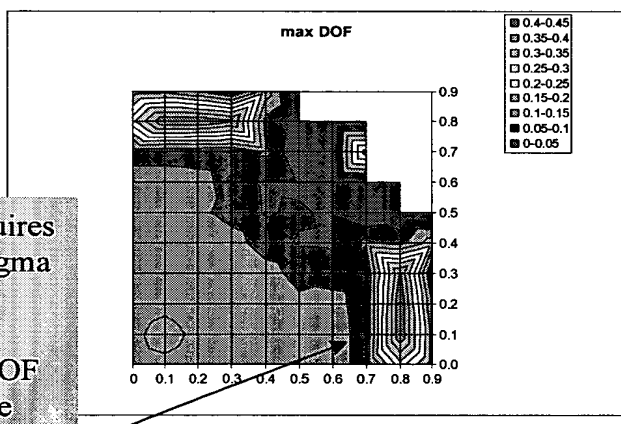



FIG. 50

6%Att-PSM



6% requires small sigma for dose latitude. Good DOF available with wide CQuad, but with poor dose latitude.

FIG. 51a

FIG. 51b

35°Cquad + 0.10σ

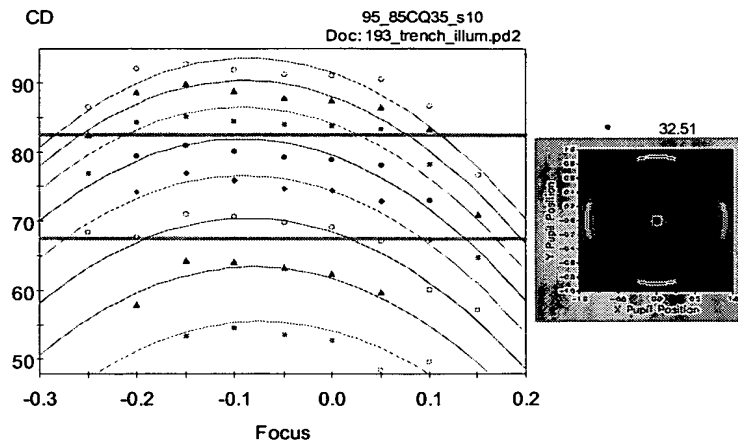


FIG. 52

Comparison of “mask assist” and “illuminator assist” for high DOF

- similar results

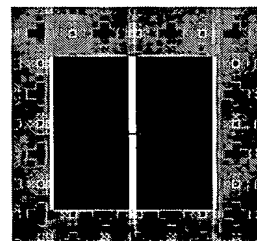
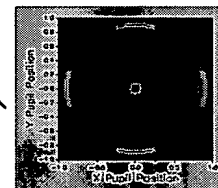
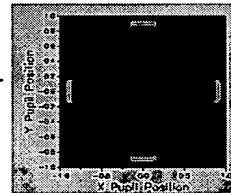
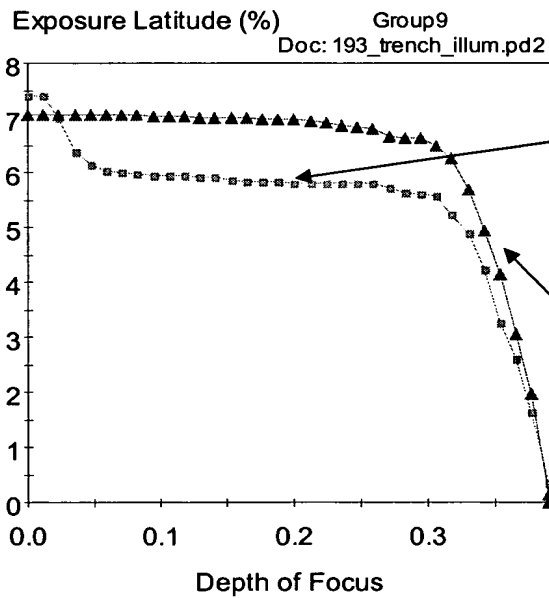


FIG. 53

Effect of bias

- Lower bias increases DOF. This is an advantage for the “simple mask, complex illuminator” case because there are no assist features to print when using low biases / high exposures.

75nm trench, variable bias
6% att-psm, 193nm 0.93NA

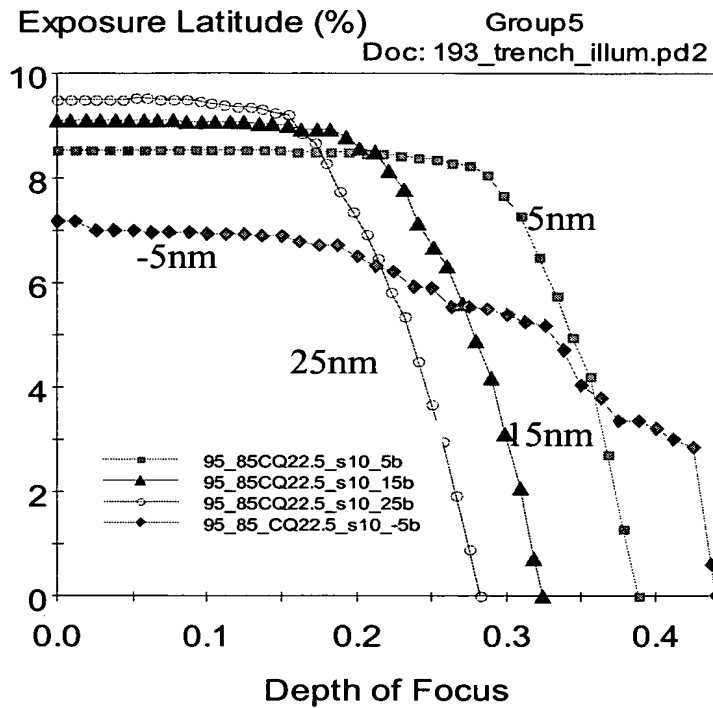
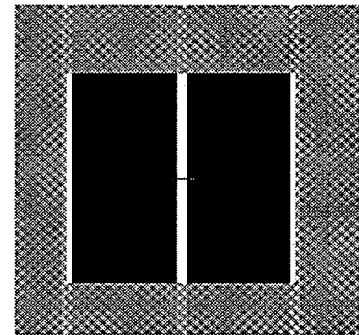
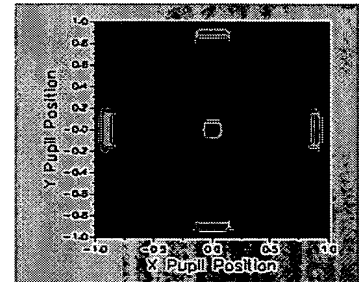


FIG.54



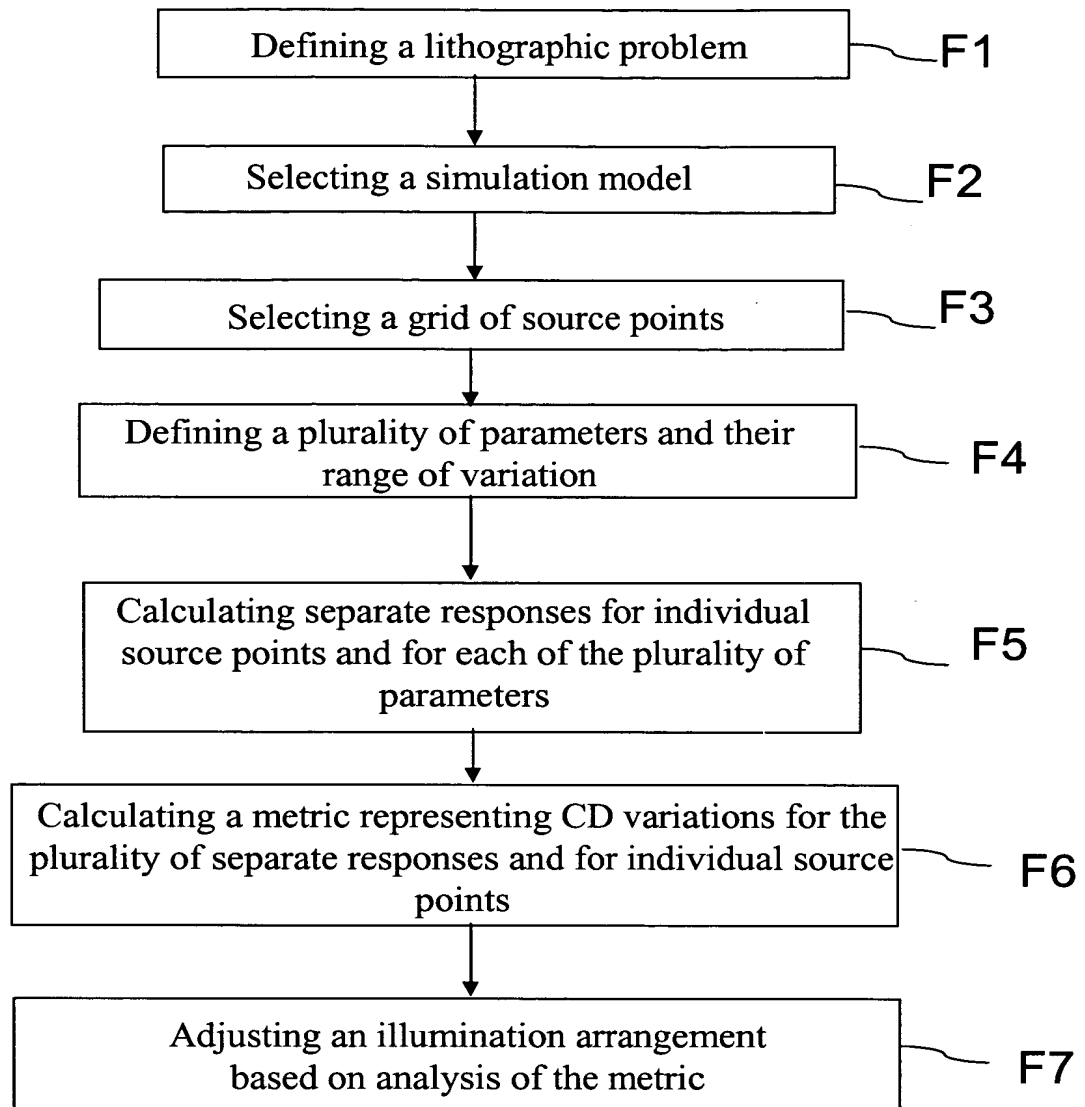
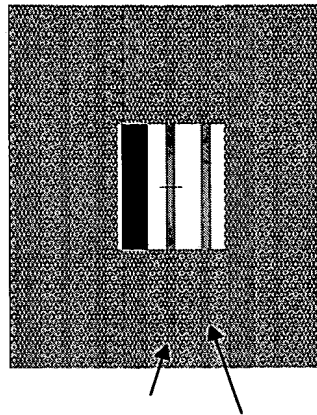


FIG. 55

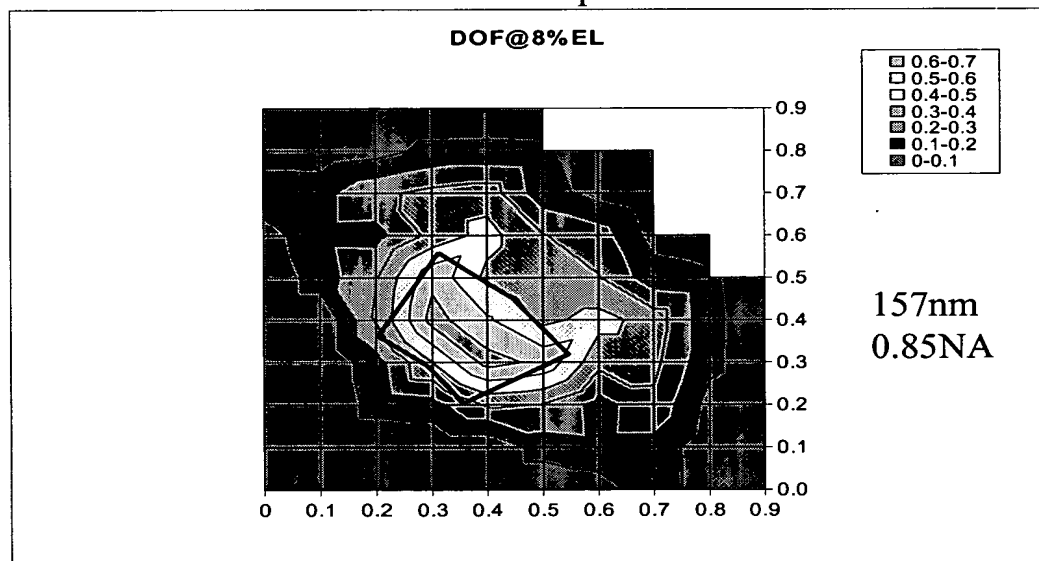
CPL for double line



Print 50nm lines

FIG. 56

Source visualization map
based on resist simulations for a grid of
source points

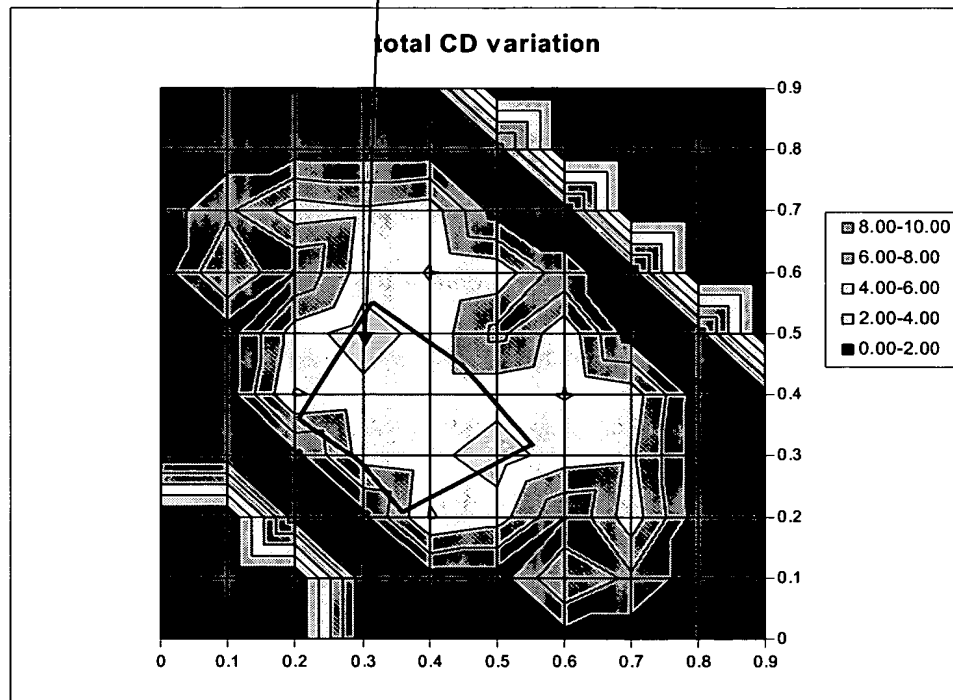


“Best choice” for illumination based on process window metric is the indicated 0.64/0.42Quasar30°.

Note: smaller poles centered at the same location expected to give better process window - larger worse.

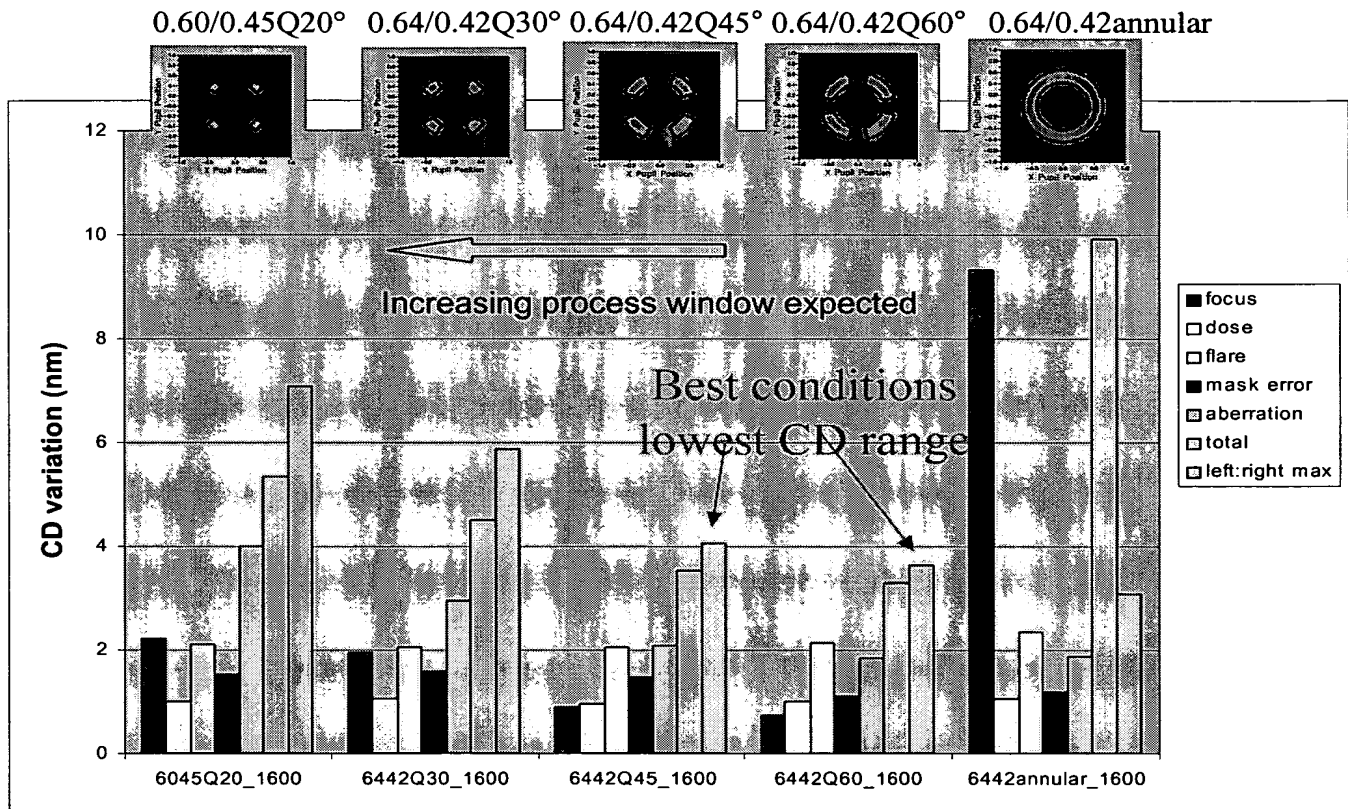
FIG. 57

Lowest CD variation (best process!) is slightly off the diagonal



Expect wider pole to improved CDU

FIG. 58



Selecting illuminator based on process window alone gives >50% more CD variation than if source visualization of CDU is included

FIG. 59